HEP-18-0197.R1

Deficient natural killer cell NKp30-mediated function and altered NCR3 splice variants in hepatocellular carcinoma

Stefania Mantovani*[1], Barbara Oliviero*[1], Andrea Lombardi[2,3], Stefania Varchetta[1], Dalila Mele[1], Angelo Sangiovanni[4], Giorgio Rossi[5], Matteo Donadon[6], Guido Torzilli[6], Cristiana Soldani[6], Camillo Porta[7], Paolo Pedrazzoli[7], Silvia Chiellino[7], Roberto Santambrogio[8], Enrico Opocher[8], Marcello Maestri[9], Stefano Bernuzzi[10], Armando Rossello[11], Sophie Clément[3], Claudio De Vito[3], Laura Rubbia-Brandt[3], Francesco Negro[3,12], Mario U Mondelli[1,2].

***Stefania Mantovani and Barbara Oliviero contributed equally to this work.**

[1]Division of Infectious Diseases and Immunology, Department of Medical Sciences and Infectious Diseases, Fondazione IRCCS Policlinico San Matteo, Pavia, Italy. [2]Department of Internal Medicine and Therapeutics, University of Pavia, Italy. [3] Division of Clinical Pathology, University Hospitals, Geneva, Switzerland. [4]CRC "A. M. and A. Migliavacca" Center for Liver Disease, Division of Gastroenterology and Hepatology and [5]Liver Transplant Unit, Fondazione IRCCS Cà Granda Ospedale Maggiore Policlinico, University of Milan, Milan, Italy. [6]Department of Hepatobiliary and General Surgery, Humanitas Clinical and Research Center, Humanitas University, Milan, Italy. [7]Medical Oncology, Fondazione IRCCS Policlinico San Matteo, Pavia, Italy.[8]Division of Gastrointestinal Surgery, San Paolo Hospital, University of Milan School of Medicine, Milan, Italy. [9]Department of General Surgery, Fondazione IRCCS Policlinico San Matteo, Pavia, Italy. [10]Immunohematological and Transfusional Service and Centre of Transplantation Immunology, Fondazione IRCCS Policlinico San Matteo, Pavia, Italy, [11] Department of Pharmacy, University of Pisa, Italy, [12]Division of Gastroenterology and Hepatology, University Hospitals, Geneva, Switzerland.

E-mails: Stefania Mantovani s.mantovani@smatteo.pv.it, Barbara Oliviero b.oliviero@smatteo.pv.it, Andrea Lombardi andrea.lombardi02@universitadipavia.it, Stefania Varchetta s.varchetta@smatteo.pv.it, Dalila Mele d.mele@smatteo.pv.it, Angelo Sangiovanni angelo.sangiovanni@policlinico.mi.it, Giorgio Rossi giorgio.rossi@unimi.it, Matteo Donadon matteo.donadon@cancercenter.humanitas.it, Guido Torzilli guido.torzilli@humanitas.it, Cristiana Soldani cristiana.soldani@humanitasresearch.it, Camillo Porta c.porta@smatteo.pv.it, Paolo Pedrazzoli p.pedrazzoli@smatteo.pv.it, Silvia Chiellino s.chiellino@smatteo.pv.it, Roberto Santambrogio roberto.santambrogio@asst-santipaolocarlo.it, Enrico Opocher enrico.opocher@unimi.it, Marcello Maestri m.maestri@smatteo.pv.it, Stefano Bernuzzi s.bernuzzi@smatteo.pv.it, Armando Rossello armando.rossello@farm.unipi.it, Sophie Clément sophie.clement@unige.ch, Claudio De Vito claudio.devito@hcuge.ch, Laura Rubbia-Brandt laura.rubbia-brandt@hcuge.ch, Francesco Negro francesco.negro@hcuge.ch, Mario U Mondelli mario.mondelli@unipv.it.

Keywords: Innate immunity, B7-H6, NKp30 isoform.

Corresponding author. Prof. Mario U. Mondelli. Address: S.C. Malattie Infettive II - Infettivologia e Immunologia, Dipartimento di Scienze Mediche e Malattie Infettive, Fondazione IRCCS Policlinico San Matteo, Piazzale Golgi 19, 27100 Pavia. Tel. +39 0382 502636; fax: +39 0382 526450. Mail: mario.mondelli@unipv.it.

Abbreviations: B7-H6, B7 homolog 6; PBMC, peripheral blood mononuclear cells; HC, healthy controls; NK, natural killer; HBV, hepatitis B virus; HCV, hepatitis C virus; HCC, Hepatocellular carcinoma; qPCR, quantitative real-time polymerase chain reaction; LIL, liver-infiltrating lymphocytes; TIL, tumor-infiltrating lymphocytes; ELISA, enzyme-linked immunosorbent assay; BCLC, Barcelona Clinic for Liver Cancer; AFP, alpha-fetoprotein; NCR, natural cytotoxicity receptor; ADAM, A Disintegrin And Metalloproteases; Tim-3, T-cell immunoglobulin and mucin-domain containing-3; FasL, Fas ligand; TIGIT, T cell immunoreceptor with Ig and ITIM domains; PD-1, programmed death receptor 1; NKG2D, natural killer group 2 member d; BAT3, HLA–B-associated transcript 3.

Financial Support: This work was supported by the Italian Ministry of Health, Bando Giovani Ricercatori, GR-2011-02349273 to BO.

Acknowledgements: AL was aided by the Nuovo-Soldati Cancer Foundation.

Abstract.

The activating natural cytotoxicity receptor NKp30 is critical for natural killer (NK) cell function and tumor immune surveillance. The natural cytotoxicity receptor-3 (NCR3) gene is transcribed into several splice variants whose physiological relevance is still incompletely understood. In this study, we investigated the role of NKp30 and its major ligand B7 homolog 6 (B7-H6) in patients with hepatocellular carcinoma (HCC). Peripheral blood NK cell phenotype was skewed toward a defective/exhausted immune profile with decreased frequencies of cells expressing NKp30 and natural killer group 2 member d (NKG2D) and an increased proportion of cells expressing T-cell immunoglobulin and mucin-domain containing-3 (Tim-3). Moreover, NKp30-positive NK cells had a reduced expression of NCR3 immunostimulatory splice variants, and an increased expression of the inhibitory variant in patients with advanced tumor, resulting in deficient NKp30-mediated functionality. Tumor-infiltrating lymphocytes showed a prevalent inhibitory NKp30 isoform profile, consistent with decreased NKp30-mediated function. Of note, there were significant differences in the cytokine milieu between the neoplastic and the surrounding non-neoplastic tissue which may have further influenced NKp30 function. Exposure of NK cells to B7-H6 expressing HCC cells significantly down-modulated NKp30, that was prevented by siRNA-mediated knockdown, suggesting a role for this ligand in inhibiting NKp30-mediated responses. Interestingly, B7-H6 expression was reduced in HCC tissue and simultaneously augmented as a soluble form in HCC patients', particularly those with advanced staging or larger nodule size. Conclusions: these findings provide evidence in support of a role of NKp30 and its major ligand in HCC development and evolution.

Introduction.

Natural killer (NK) cells play a significant role in innate immune responses to cancer cells via recognition of germline-encoded ligands of positive and negative signaling receptors. Lysis of tumor targets occurs through reduction of inhibitory signals and a simultaneous increase in

activating signals that are necessary for NK cell triggering [1-3]. Activating receptors include DNAM-1, NKG2D, and the natural cytotoxicity receptors (NCR), whose ligands comprise both MHC-like and non-MHC molecules. The NCR family includes NKp30 (NCR3), NKp44 (NCR2) and NKp46 (NCR1) which are type I transmembrane glycoproteins comprising one (NKp30 and NKp44) or two (NKp46) Ig-like extracellular domains [4]. The NCR3 gene is transcribed into three major isoforms (NKP30a, NKp30b and NKp30c) of the NKp30 protein that are generated by alternative splicing and that have different biological functions. The NKp30a and NKp30b isoforms are considered immunostimulatory as they induce cytotoxicity and Th1 cytokine secretion, respectively, while the NKp30c isoform shows an immunosuppressive activity triggering IL-10 release. Furthermore, the relative abundance of the mRNA encoding the NKp30c isoform compared to isoform a or b can negatively impact on the prognosis and evolution of different malignancies and might be associated with advanced liver disease in HCV-infected patients [5-8]. Moreover, the expression of different NCR3 splice variants by NK cells delineates functionally distinct subsets and is governed by the cytokine-defined microenvironment [9,10]. The NKp30 receptor recognizes the HLA–B-associated transcript 3 (BAT3), the human cytomegalovirus pp65 tegument protein and the cell surface protein B7 homolog 6 (B7-H6), a member of the B7 family of receptors [11-13]. Interestingly, B7-H6 is not expressed by normal human tissues but is selectively expressed on stressed cells, including both solid and transformed blood cells, which can up-regulate B7-H6 expression and enhance tumor susceptibility to NK cell lysis [14-16]. The interaction of B7-H6 on tumor cells with NKp30 on NK cells results in interferon-γ (IFN-γ) production and tumor cell killing, suggesting that the NKp30–B7-H6 axis can be exploited for cancer immunotherapy [17]. In addition, B7-H6 can also be induced as a stress protein by viral infections closely linked to carcinogenesis such as hepatitis B virus (HBV) [18]. Current evidence indicates that malignant cells can also bypass the NK surveillance by releasing B7-H6 as soluble proteins that block NKp30 activity, suggesting that this may be an immune escape mechanism of tumor cells from NK cell-mediated killing [19]. It is clear from the aforementioned that the NKp30-B7H6 axis represent an

important pathway in chronic inflammation proceeding to tumor development. One such example is hepatocellular carcinoma (HCC) which may develop in the setting of advanced chronic hepatitis B (HBV) and chronic hepatitis C (HCV) virus infections [20].

In this study we have investigated the NKp30-B7-H6 axis in patients with HCC. We showed that peripheral and tumor-infiltrating NKp30+ NK cells have deficient NKp30-mediated functionality and altered expression of NCR3 splice variants. Moreover, B7-H6 expression was reduced in HCC tissue and simultaneously augmented as a soluble form in the serum of HCC patients, particularly those with advanced staging or larger nodule size. These findings provide evidence in support of a role of NKp30 and its major ligand in HCC development and evolution.

Materials and Methods.

Complete technical details are reported in Supplementary Materials and Methods. Briefly, paired blood and tissue infiltrating lymphocytes were obtained from patients undergoing surgical liver resections for HCC (Supplementary Table 1) and prepared for phenotype determination and redirected functional analysis via NKp30 ligation, RNA extraction and qPCR to detect NKp30 isoforms. Primary HCC cell cultures were established as described in Supplementary M&M. Liver samples from HCC and cirrhotic patients were retrospectively examined as described in Supplementary M&M. NKp30 down-regulation experiments using B7-H6 expressing cells and B7-H6 siRNA knock-down are also described in Supplementary M&M.

Statistical analysis was performed using the GraphPad Prism 6 software. The non-parametric Wilcoxon matched-pairs signed rank test or Mann-Whitney U test as well as parametric paired or unpaired t test were used as appropriate. The Dunn's multiple comparison test was used to compare more than two groups of data. Pearson test was used to examine correlations. A p value ≤ 0.05 was deemed statistically significant.

Results.

Peripheral NK cells show an exhausted phenotype in HCC patients and NKp30-expressing NK cells are enriched in tumor-infiltrating lymphocytes.

We investigated the frequency of circulating NK cells in HCC patients and HC, according to the gating strategy shown in Supplementary fig. 1, and found that frequencies of total peripheral NK cells and of the $CD56^{bright}$ and $CD56^{dim}$ subsets (Fig. 1A) were comparable in HCC patients and HC. The frequency of peripheral NK cells carrying NKp30 receptor and its expression were instead significantly lower in patients with HCC compared to HC (Fig. 1B-C). There were no differences in NKp30 expression according to liver disease etiology (not shown). The frequency of the immunomodulatory T-cell immunoglobulin- and mucin-domain-containing molecule-3 (Tim-3) receptor was significantly higher in HCC patients' NK cells, compared to HC NK cells (Fig. 1D). Moreover, there was a statistically significant reduction in the proportion of NKG2D+ (Fig. 1E) and a significant increase in the proportion of CD69+ (Fig. 1F) NK cells from patients with HCC compared with controls. At the same time, no statistically significant differences were noted in the proportion of programmed death receptor 1 (PD-1), NKG2A, Fas ligand (FasL), T cell immunoreceptor with Ig and ITIM domains (TIGIT) and NKp46 (Supplementary Fig 2A-E) expressing NK cells compared to HC. We further investigated intrahepatic NK cell receptors in HCC patients and found a lower frequency of total NK cells in TIL compared to LIL (Fig. 2A), as shown by others [21, 22]. However, the proportion of NKp30+ NK cells and the mean fluorescence intensity (MFI) of the NKp30 receptor were significantly higher in TIL- compared with LIL-NK cells (Fig. 2B-D). There was a higher frequency of NKp30+ NK cells in the $CD56^{bright}$ subset in TIL compared with LIL (Fig. 2E). In contrast, the proportion of NKp46+ NK cells and the NKp46 MFI were similar in tumor and non-tumor NK cells (data not shown).

Deficient NKp30-mediated functionality and altered NKp30 isoform profile in HCC patients.

Altered expression of NKp30 receptor in HCC patients prompted us to study the NKp30-mediated cytolytic potential and cytokine production of peripheral and intrahepatic NK cells of HCC patients, using an *ex vivo* redirected functional (ADCC) assay. PBMC, TIL and matched LIL were incubated overnight with or without IL15 and subsequently co-cultured with the FcγR+ P815 murine cell line in the presence of anti-NKp30 mAb. Patients with chronic HCV infection without HCC were added as disease controls. There was no difference in peripheral NKp30-mediated cytotoxicity between patients with HCC, patients with chronic HCV infection and HC (Fig. 3A). NKp30 expression was reduced in the HCV+ disease control group (not shown) compared to HC, in keeping with previously published data from our laboratory [8]. After IL15 stimulation, NKp30-mediated cytotoxicity was significantly augmented in HCV+ patients compared to HC, whereas HCC patients displayed a lower cytotoxic potential compared to HCV+ patients (Fig. 3A). NKp30-mediated IFN-γ production was significantly reduced in peripheral blood NK cells from both HCC and HCV+ patients compared to HC, which was maintained in HCC patients also after IL15 stimulation (Fig. 3B). There was a trend toward a more profound reduction in IFNγ secretion for HCC patients compared to non-HCC, HCV+ controls (Fig. 3B). The NKp30-mediated functional dichotomy exhibited by peripheral blood NK cells in chronic HCV infection, i.e. increased degranulation and poor cytokine production, is consistent with previous findings from our own and other laboratories [23, 24].

When we analyzed the intrahepatic compartment, we found that the NKp30-mediated degranulation ability of TIL-NK cells tested by reverse ADCC was significantly reduced compared with matched LIL-NK cells (Fig. 3C). IL15 stimulation was unable to rescue NKp30-mediated degranulation in TIL-NK cells, despite being able to boost NKp30 expression (data not shown). No statistically significant differences in IFN-γ (and TNFα, not shown) production were noted following NKp30 ligation (Fig. 3D).

Recent studies have shown that the NKp30 isoform expression pattern affects the NK cell functionality, the prognosis and evolution in the settings of cancer and infection [6-8]. We

183 investigated whether alternatively spliced variants of the NCR3 gene might explain the reduced
184 NKp30-mediated cytokine production of peripheral blood NK cells in HCC patients. To this end,
185 we quantified the three major NKp30 isoforms (NKp30a, b and c) in freshly isolated PBMC of
186 patients and HC using qPCR. The relative expression of the immunostimulatory NKp30a and
187 NKp30b isoforms was significantly lower in HCC patients than in HC (Fig. 4A). In agreement with
188 the low NKp30a and b transcripts, the Δac and Δbc ratio values were lower in NK cells from
189 patients with HCC compared to HC (Fig. 4B). Interestingly, when HCC patients were analyzed
190 according to the Barcelona Clinic for Liver Cancer (BCLC) staging classification, we found that the
191 immunosuppressive NKp30c isoform was increased in patients with advanced tumor (Fig. 4C).
192 Notably, there was a statistically significant positive correlation between the NKp30 a/c isoform
193 ratio and IFNγ by NK cells, providing further evidence in support of the immunostimulatory
194 function of the NKp30a isoform (Fig. 4D).
195 In consideration of the inhibitory function of NKp30 [25] and the potential role of microenvironment
196 cytokines in influencing the NCR3 splice variants [9], we explored whether a switched NKp30
197 isoform profile could explain the deficient degranulation efficiency of TIL-NK cells in HCC
198 patients. To this end, we quantified the three major NKp30 isoforms in freshly isolated LIL and
199 matched TIL-NK cells. As shown in fig. 4E, the relative expression of the immunostimulatory
200 NKp30b isoforms was significantly lower in TIL-NK cells than in LIL-NK cells. TIL-NK cells
201 exhibited a reduced Δbc ratio compared to the matched non-tumor liver counterpart, suggesting a
202 prevalent inhibitory NKp30-mediated signaling (Fig. 4F). This difference in tissue-specific NKp30
203 isoform profile and NK cell functionality prompted us to examine changes in the cytokine content
204 in the neoplastic and the surrounding non-neoplastic liver tissue. To this end, we analyzed mRNAs
205 of selected cytokines that were previously shown to be involved in the necroinflammatory process
206 leading to advanced fibrosis and liver carcinogenesis [26-31], as well as in NK cell regulation [32].
207 There was a reduced mRNA content of certain cytokines, including IL-6, IL-8 and IL-10, in the

tumor compared with the non-neoplastic tissue, whereas no statistically significant differences were observed for IL-18 and TGF-β mRNAs (Fig. 5).

NKp30 receptor is downregulated after exposure to B7-H6 expressing HCC cells.

To assess whether NKp30 expression could be influenced by B7-H6 contact we performed co-culture experiments with hepatocellular carcinoma Huh7.5 cell line expressing the B7-H6 ligand. As shown in fig. 6A, B7-H6 expression was higher on HCV-infected Huh7.5 cells than on uninfected cells. The frequency of NK cells carrying the NKp30 receptor and its expression were downregulated after exposure of PBMC from HC to uninfected Huh7.5 cells, expressing low levels of B7-H6. A stronger downregulation was shown when PBMC were incubated with HCV-infected Huh7.5 cells, expressing higher levels of B7-H6, both as percentage and MFI (Fig. 6B-C). In contrast, NKp46 expression remained unchanged (data not shown). Representative dot plots showing NKp30+ and NKp46+ NK cell frequencies after B7-H6 exposure are shown in supplementary 3. B7-H6-induced NKp30 downregulation was also confirmed by siRNA-mediated knockdown. Surface B7-H6 expression was evaluated on HepG2 cells after transfection with B7-H6- and or negative control-siRNA by flow cytometry and qPCR (Fig. 6D and Fig. 4S). As shown in fig. 6D, siRNA-mediated knockdown of B7-H6 was able to reduce B7-H6 expression in HepG2 cells. The frequency of NK cells carrying the NKp30 receptor and its expression were higher after exposure of PBMC from HC to siRNA-B7-H6-transfected HepG2 cells compared to siRNA-negative control (Fig. 6E-F). B7-H6-induced NKp30 downregulation was also confirmed after PBMC exposure to the breast carcinoma cell lines MCF-7/VC or MCF-7/B7-H6, retrovirally transduced with pMXneo or pMXneo-CD8L-Myc tag-B7-H6, respectively (Fig. 5S). Furthermore, to assess whether NKp30 expression could be influenced by soluble B7-H6 (sB7-H6) we performed experiments incubating PBMC from HC with heterologous HC's serum and HCC patients' serum. No statistically significant differences were observed, suggesting that NKp30 down-regulation requires B7-H6 to be cell-associated (Supplementary Fig. 6).

B7-H6 protein expression is reduced in tumor tissue of HCC patients.

Expression of the NKp30 ligand B7-H6 was evaluated in HCC biopsy specimens by immunohistochemistry and compared to cirrhotic livers. B7-H6 was highly expressed in cirrhotic livers and was significantly less expressed in HCC tissue stratified according to the degree of differentiation: well-, moderately- and poorly-differentiated tissue (Fig. 7A). Interestingly, we found that poorly-differentiated tumor cells showed a trend toward lower B7-H6 expression compared to better differentiated HCC tissues. Immunohistochemical staining showed that B7-H6 was mainly localized in the cytoplasm and on the membrane of hepatocytes as shown in fig. 7B. To investigate whether different levels of B7-H6 protein expression by immunohistochemistry *in situ* were caused by a decrease in gene transcription, we analysed B7-H6 mRNA levels in HCC tissues along with matched non-tumor specimens but we were unable to detect significant differences (Fig. 7C), suggesting that decreased B7-H6 protein expression did not result from reduced transcript levels, and might have occurred via other post-transcriptional mechanisms. Schlecker et al. demonstrated a novel mechanism of immune escape in which tumor cells impede NK cell recognition by metzincin-mediated shedding of B7-H6 [(33)]. To address whether this mechanism plays a role in B7-H6 downregulation on HCC patients we treated HCC primary cell lines with different ADAM-specific inhibitors. B7-H6 surface expression was measured by flow cytometry on untreated HCC primary cell lines or after exposure to ADAM-10 and ADAM-17 inhibitors LT4 or MN8 or to solvent alone (DMSO) for 24 h. As shown in Supplementary fig. 7, there was a modest and not always consistent increase in B7-H6 surface expression only after exposure of HCC cells to MN8.

Soluble B7-H6 serum concentrations are elevated in HCC patients with intermediate and advanced tumors and correlate with clinical parameters.

Based on *in situ* expression of B7-H6 in HCC, we next investigated whether sB7-H6 was detectable in patients' sera by ELISA. As shown in fig. 8A, higher serum B7-H6 levels were detected in HCC patients with intermediate and advanced tumor, classified according to the BCLC staging classification, compared to early stage tumors (BCLC-A) and to HC and cirrhotic patients. Differences between HC, cirrhosis and HCC remained highly significant when HCC were not stratified according to BCLC stage (not shown). There were no significant differences in sB7-H6 levels when HCC patients were stratified according to etiology or tumor grading (data not shown). Moreover, there were positive correlations between sB7-H6 levels and HCC nodule size and serum alpha fetoprotein values (Fig. 8B and C).

Discussion.

Functional deficiencies of circulating and intrahepatic NK cells have been demonstrated in various human cancers including hepatocellular carcinoma [21, 22, 25, 34, 35]. Nevertheless, the mechanisms responsible for altered NK cell effector function and their association with disease progression remain largely unexplored. Previous studies found a reduction in the proportion of peripheral blood NK cells and of $CD56^{dim}$ phenotype in HCC patients [21, 22, 35] which could contribute to reduced immune surveillance, whereas no differences were found in our study between patients and controls. These discrepancies might be a consequence of patient selection, since our patients had an overall more advanced disease, a larger proportion of them being categorized as BCLC-B, C, D, whereas the vast majority of patients in Cheung et al.[22] and Cariani et al.[35] were classified as BCLC-A. An altered NK cell phenotype may reflect NK cell anergy which, however, does not always correlate with altered expression of activating and inhibitory receptors on NK cells in HCC patients. Relevant to this statement, there are controversial data regarding the frequencies of NK

cells carrying NKG2D and NKG2A receptors in circulating and intrahepatic NK cells [21, 22, 35]. Interestingly, phenotypic analysis of our patients with HCC showed decreased frequencies of NK cells expressing NKp30 and NKG2D activating receptors, together with an increased frequency of Tim-3, suggesting that innate immunity is skewed toward exhausted anti-tumor immune responses despite of an increased proportion of NK cells expressing the CD69 early activation marker. Recent studies have reported conflicting data about Tim-3 function in NK cells [36-38]. Ndhlovu and colleagues showed that Tim-3 inhibits NK cell–mediated cytotoxicity [36], whereas another study suggested that Tim-3 may instead enhance IFN-γ production [37]. Both studies focused on healthy donors and not patients with chronic diseases, such as cancer. In cancer patients, da Silva and colleagues showed that Tim-3 could function as an NK-cell exhaustion marker in advanced melanoma and that its blockade reverses the NK exhausted phenotype [38]. Functional NK cell deficiency might be also associated with an increased regulatory T cell frequency, an altered dendritic cell function and an increased proportion of myeloid-derived suppressor cells [21, 25, 39]. Apart from those mechanisms, alternative splicing of the NCR3 gene has been shown to profoundly influence NKp30-dependent function and it has been correlated with the prognosis and evolution in gastrointestinal stromal tumor patients, as well as other cancers, viral infections and miscarriage [5-10]. However, no information is currently available on NCR3 splice variant profile and function in liver cancer. In the present study we showed that in HCC patients NK cells displayed reduced NKp30 expression, as well as NKp30-mediated cytokine secretion and cytotoxicity. We also showed, for the first time, that peripheral and tumor infiltrating NKp30-expressing NK cells displayed altered expression of the major NKp30 isoforms (NKp30a, NKp30b and NKp30c), which is compatible with defective NKp30-mediated tumor immune surveillance in HCC patients. Indeed, PBMC of HCC patients displayed a lower mRNA expression level of the NKp30a and b immunostimulatory isoforms compared to HC and in those patients with advanced tumor, expression of the inhibitory NKp30c isoform was clearly increased. Furthermore, NK cells displaying a reduced NKp30 a/c isoform ratio exhibited a reduced NKp30-mediated cytokine

production. Moreover, considering the relative expression of the different NCR3 alternative splice variants, there was a bias toward a prevalent inhibitory NKp30 isoform profile in the liver compartment, consistent with decreased NKp30-mediated function. The aforementioned shed new light on the role for the NKp30 receptor in HCC surveillance. In line with this interpretation, NKp30-mediated cytokine production by circulating NK cells was found to be reduced in HCC patients compared with controls, in keeping with a lower frequency of NKp30+ NK cells and a lower density of NKp30 receptor expression in HCC compared with HC. These findings somehow differ from those obtained in the intrahepatic compartment in which NKp30-mediated NK cell degranulation was reduced despite higher relative frequency of NKp30+ cells and higher density of the NKp30 receptor in neoplastic compared with non-neoplastic adjacent tissues. In this respect, NKp30-mediated responses may be influenced by differences in the cytokine milieu between the neoplastic and non-neoplastic tissue, as shown in previous studies supporting an epigenetic role for certain cytokines, such as TGF-β, IL-15 and IL-18, that are enriched in a specific microenvironment, to convert the NCR3 splice variant profile of NK cells and to affect the NK cytolytic behavior [9, 10]. In line with these findings, our data showing a reduced pro-inflammatory cytokine (IL-6, IL-8) mRNA content and a concomitant inhibitory signal delivered by unaltered TGF-β mRNA expression in the neoplastic tissue, support the existence of an inhibitory microenvironment affecting NK cell responses. Thus, the evidence gathered in this study pointed to peculiar characteristics of the neoplastic tissue in patients with HCC, in whom the NKp30 isoform analysis was compatible with an inhibitory profile, despite an increased relative proportion of NKp30 positive NK cells.

Our data clearly emphasized the role of B7-H6 in regulating NKp30 expression. Interaction of B7-H6 with NKp30 on NK cells leads to efficient NK cell activation and target cell killing [40]. The absence of B7-H6 transcripts in normal tissues and the presence in tumor cells, on inflammatory monocytes during sepsis and in viral infections, define B7-H6 as an example of a stress-induced self molecule [18, 41, 42]. Until now, hepatic B7-H6 expression remained poorly explored. Zou et al.

investigated B7-H6 protein expression on HBV-induced acute on chronic liver failure and another study showed B7-H6 expression at the transcriptional level in hepatocellular carcinoma [18, 43]; however, the non-neoplastic liver was only poorly explored. In the former study, B7-H6 expression, assessed by immunohistochemistry, was found to be markedly enhanced on HBV-infected hepatocytes compared to the healthy liver and its expression positively correlated with the severity of liver injury in this clinical setting [18]. In addition, Fiegler et al. observed elevated B7-H6 mRNA levels in HCC tissue compared to normal liver controls [43]. Importantly, our results compared tumor tissue and cirrhotic liver showing a significantly reduced B7-H6 expression in HCC tissue by immunohistochemistry. Notably, the HCC tissue exhibited different intensity of B7-H6 expression according to tumor differentiation status, the ligand being less expressed, though not significantly so, in poorly differentiated HCC. Decreased B7-H6 expression was not caused by altered gene transcription, since tumor B7-H6 mRNA levels were not significantly different from those of the surrounding non-neoplastic tissue, suggesting that other mechanisms might be involved. Similarly to other members of the B7 family, B7-H6 was also identified in a soluble form capable of binding to NKp30 receptor and to prevent NKp30-mediated NK cell triggering. Release of sB7-H6 was shown to be at least in part compatible with a metzincin-mediated shedding mechanism, since ADAM-specific inhibitors slightly increased B7-H6 surface expression on primary HCC cell lines, in agreement with data in melanoma patients [33]. The role of soluble B7-H6 in HCC is not entirely clear, since a short incubation with heterologous serum containing cell-free B7-H6 was unable to decrease the proportion of NKp30+ NK cells *in vitro*, whereas cell-associated B7-H6 clearly was. Instead, a competing role for B7-H6 has convincingly been shown in ovarian carcinoma in which down-modulation of the NKp30 receptor expression and function on tumor-associated NK cells were associated with the presence of its ligand B7-H6 as a surface/cytosolic molecule in tumor cells as well as a soluble molecule [19]. In line with this observation, and in agreement with our data showing a clear ligand-induced receptor down-modulation, higher NKp30 expression observed in TIL compared to LIL may be due to an absent down-regulatory effect caused by reduced ligand-

receptor interaction. Evidence in support of this hypothesis comes from our data showing decreased expression of B7-H6 ligand in HCC tissues. Moreover, significantly elevated levels of sB7-H6 were detected in sera of HCC patients with intermediate and advanced tumor compared with healthy controls and cirrhotic patients, suggesting a potential inhibitory role for this soluble ligand on NKp30 expression and NKp30-mediated NK cell activity. Our data suggesting that B7-H6 is released by sheddases from neoplastic cells are compatible with larger amounts of soluble ligand being shed from larger neoplastic nodules or advanced HCC. This may represent an evasion mechanism from the host immune surveillance.

In conclusion, our study provides evidence in support of an alteration of the NKp30/B7-H6 axis in HCC and reveals several mechanisms that can be exploited for novel immunotherapeutic approaches for liver cancer. It may be envisaged that beyond restoring cytotoxic T lymphocyte activity with checkpoint inhibitors, such as PD-1/PD-L1-specific monoclonal antibodies [(44)], it could also be possible to associate specific immune interventions to modulate altered NK cell activity. Also, it is of interest that sorafenib, which for years was the only systemic treatment available for patients with advanced HCC [(45)], primes proinflammatory responses of macrophages located within the HCC microenvironment and induces anti-tumor NK cell responses in a cytokine-dependent fashion, providing new insights for immune stimulatory treatments [(46)].

References

1) Morvan MG, Lanier LL. NK cells and cancer: you can teach innate cells new tricks. Nat Rev Cancer 2016;16:7-19.
2) Lanier, LL. Up on the tightrope: natural killer cell activation and inhibition. Nat. Immunol 2008;9:495–502.

3) Long EO, Kim HS, Liu D, Peterson ME, Rajagopalan S. Controlling natural killer cell responses: integration of signals for activation and inhibition. Annu Rev Immunol 2013;31:227-58

4) Kruse PH, Matta J, Ugolini S, Vivier E. Natural cytotoxicity receptors and their ligands. Immunol Cell Biol 2014;92:221-9.

5) Messaoudene M, Fregni G, Enot D, Jacquelot N, Neves E, Germaud N, et al. NKp30 isoforms and NKp46 transcripts in metastatic melanoma patients: Unique NKp30 pattern in rare melanoma patients with favorable evolution. Oncoimmunology 2016;5: e1154251.

6) Semeraro M, Rusakiewicz S, Minard-Colin V, Delahaye NF, Enot D, Vély F et al. Clinical impact of the NKp30/B7-H6 axis in high-risk neuroblastoma patients. Sci Transl Med 2015;7:283ra55.

7) Delahaye NF, Rusakiewicz S, Martins I, Menard C, Roux S, Lyonnet L, et al. Alternatively spliced NKp30 isoforms affect the prognosis of gastrointestinal stromal tumors. Nat Med 2011;17:700-7

8) Mantovani S, Mele D, Oliviero B, Barbarini G, Varchetta S, Mondelli MU. NKp30 isoforms in patients with chronic hepatitis C virus infection. Immunology 2015;146:234-42.

9) Siewiera J, Gouilly J, Hocine H, Cartron G, Levy C, Al-Daccak R, et al. Natural cytotoxicity receptor splice variants orchestrate the distinct functions of human natural killer cell subtypes. Nat Commun 2015;6:10183

10) Shemesh A, Tirosh D, Sheiner E, Benshalom-Tirosh N, Brusilovsky M, Segev R, et al. First Trimester Pregnancy Loss and the Expression of Alternatively Spliced NKp30 Isoforms in Maternal Blood and Placental Tissue. Frontiers in Immunology 2015;6:189.

11) Pogge von Strandmann E, Simhadri VR, von Tresckow B, Sasse S, Reiners KS, Hansen HP, et al. Human leukocyte antigen-B-associated transcript 3 is released from tumor cells and engages the NKp30 receptor on natural killer cells. Immunity 2007;27:965–974.

12) Arnon TI, Achdout H, Levi O, Markel G, Saleh N, Katz G, et al. Inhibition of the NKp30 activating receptor by pp65 of human cytomegalovirus. Nat Immunol 2005;6:515–523

13) Brandt CS, Baratin M, Yi EC, Kennedy J, Gao Z, Fox B, et al. The B7 family member B7-H6 is a tumor cell ligand for the activating natural killer cell receptor NKp30 in humans. J Exp Med 2009;206:1495-503.

14) Sun J, Tao H, Li X, Wang L, Yang J, Wu P, et al. Clinical significance of novel costimulatory molecule B7-H6 in human breast cancer. Oncol Lett 2017;14:2405-2409.

15) Wang J, Jin X, Liu J, Zhao K, Xu H, Wen J, et al. The prognostic value of B7-H6 protein expression in human oral squamous cell carcinoma. J Oral Pathol Med 2017; 6:766-772

16) Jiang T, Wu W, Zhang H, Zhang X, Zhang D, Wang Q, et al. High expression of B7-H6 in human glioma tissues promotes tumor progression. Oncotarget 2017;8:37435-37447

17) Chester C, Fritsch K, Kohrt H.E. Natural killer cell immunomodulation: targeting activating, inhibitory, and co-stimulatory receptor signaling for cancer immunotherapy. Front Immunol 2015;6: 601

18) **Zou Y, Bao J**, Pan X, Lu Y, Liao S, Wang X, et al. NKP30-B7-H6 Interaction Aggravates Hepatocyte Damage through Up-Regulation of Interleukin-32 Expression in Hepatitis B Virus-Related Acute-On-Chronic Liver Failure. PLoS One 2015;10:e0134568.

19) **Pesce S, Tabellini G**, Cantoni C, Patrizi O, Coltrini D, Rampinelli F, et al. B7-H6-mediated downregulation of NKp30 in NK cells contributes to ovarian carcinoma immune escape. Oncoimmunology 2015;4:e1001224.

20) Takeda H, Takai A, Inuzuka T, Marusawa H. Genetic basis of hepatitis virus-associated hepatocellular carcinoma: linkage between infection, inflammation, and tumorigenesis. J Gastroenterol 2017;52:26-38.

21) **Cai L, Zhang Z**, Zhou L, Wang H, Fu J, Zhang S, et. al. Functional impairment in circulating and intrahepatic NK cells and relative mechanism in hepatocellular carcinoma patients. Clin Immunol 2008;129:428-37.

22) Cheung PF, Yip CW, Ng LW, Wong CK, Cheung TT, Lo CM, et al. Restoration of natural killer activity in hepatocellular carcinoma by treatment with antibody against granulin-epithelin precursor. Oncoimmunology 2015;4:e1016706

23) **Oliviero B, Varchetta S**, Paudice E, Michelone G, Zaramella M, Mavilio D, et al. Natural killer cell functional dichotomy in chronic hepatitis B and chronic hepatitis C virus infections. Gastroenterology 2009;137:1151-1160

24) Ahlenstiel G, Titerence RH, Koh C, Edlich B, Feld JJ, Rotman Y et al. Natural killer cells are polarized toward cytotoxicity in chronic hepatitis C in an interferon-alfa-dependent manner. Gastroenterology 2010; 138:325-35.

25) **Hoechst B, Voigtlaender T**, Ormandy L, Gamrekelashvili J, Zhao F, Wedemeyer H, et al. Myeloid derived suppressor cells inhibit natural killer cells in patients with hepatocellular carcinoma via the NKp30 receptor. Hepatology 2009;50:799-807

26) Chia CS, Ban K, Ithnin H, Singh H, Krishnan R, Mokhtar S et al. Expression of interleukin-18, interferon-gamma and interleukin-10 in hepatocellular carcinoma. Immunol Lett 2002;84:163-72.

27) Markowitz1 GJ, Yang P, Fu J, Michelotti GA, Chen R, Sui J et al. Inflammation-Dependent IL18 signaling restricts hepatocellular carcinoma growth by enhancing the accumulation and activity of tumor infiltrating lymphocytes. Cancer Res 2016;76:2394–2405.

28) Budhu A, Forgues M, Ye QH, Jia HL, He P, Zanetti KA et al. Prediction of venous metastases, recurrence, and prognosis in hepatocellular carcinoma based on a unique immune response signature of the liver microenvironment. Cancer Cell 2006;10:99–111.

29) Massague J. TGFbeta in Cancer. Cell 2008;134:215–230.

30) **Hernandez-Gea V, Toffanin S**, Friedman SL, Llovet JM. Role of the microenvironment in the pathogenesis and treatment of hepatocellular carcinoma. Gastroenterology 2013;144:512-27.

31) Bataller R, Brenner DA. Liver fibrosis. J Clin Invest 2005;115:209–218.

462 32) Vivier E, Tomasello E, Baratin1 M, Walzer T & Ugolini S. Functions of natural killer cells.
463 Nat Immunol 2008;9:503-10
464 33) Schlecker E, Fiegler N, Arnold A, Altevogt P, Rose-John S, Moldenhauer G, et al.
465 Metalloprotease-mediated tumor cell shedding of B7-H6, the ligand of the natural killer cell-
466 activating receptor NKp30. Cancer Res 2014;74:3429-40.
467 34) Sun C, Xu J, Huang Q, Huang M, Wen H, Zhang C, et al. High NKG2A expression
468 contributes to NK cell exhaustion and predicts a poor prognosis of patients with liver cancer.
469 Oncoimmunology 2016;6:e1264562.
470 35) Cariani E, Pilli M, Barili V, Porro E, Biasini E, Olivani A et al. Natural killer cells
471 phenotypic characterization as an outcome predictor of HCV-linked HCC after curative
472 treatments. Oncoimmunology 2016;5:e1154249.
473 36) Ndhlovu LC, Lopez-Verges S, Barbour JD, Jones RB, Jha AR, Long BR, et al. Tim-3 marks
474 human natural killer cell maturation and suppresses cell-mediated cytotoxicity. Blood
475 2012;119:3734–43.
476 37) Gleason MK, Lenvik TR, McCullar V, Felices M, O'Brien MS, Cooley SA, et al. Tim-3 is
477 an inducible human natural killer cell receptor that enhances interferon gamma production in
478 response to galectin-9. Blood 2012;119:3064–72
479 38) da Silva IP, Gallois A, Jimenez-Baranda S, Khan S, Anderson AC et al. Reversal of NK-cell
480 exhaustion in advanced melanoma by Tim-3 blockade. Cancer Immunol Res. 2014;2:410-
481 22.
482 39) Ormandy LA, Farber A, Cantz T, Petrykowska S, Wedemeyer H, et al. Direct ex vivo
483 analysis of dendritic cells in patients with hepatocellular carcinoma. World J Gastroenterol
484 2006;12:3275-82.
485 40) Kaifu T, Escaliere B, Gastinel LN, Vivier E, Baratin M. B7-H6/NKp30 interaction: a
486 mechanism of alerting NK cells against tumors. Cell Mol Life Sci 2011;68:3531– 9.

41) Matta J, Baratin M, Chiche L, Forel J, Farnarier C, Piperoglou C, et al. Induction of B7-H6, a ligand for the natural killer cell-activating receptor NKp30, in inflammatory conditions. Blood 2013;122:394-404.

42) Schmiedel D, Tai J, Levi-Schaffer F, Dovrat S, Mandelboim O. Human Herpesvirus 6B Downregulates Expression of Activating Ligands during Lytic Infection To Escape Elimination by Natural Killer Cells. J Virol 2016;90:9608-9617.

43) Fiegler N, Textor S, Arnold A, Rölle A, Oehme I, Breuhahn K et al. Downregulation of the activating NKp30 ligand B7-H6 by HDAC inhibitors impairs tumor cell recognition by NK cells. Blood 2013;122:684-93.

44) Greten TF, Sangro B. Targets for immunotherapy of liver cancer. Journal of Hepatology 2017;68:157-166.

45) Llovet JM, Ricci S, Mazzaferro V, Hilgard P, Gane E, Blanc JF et al. Sorafenib in advanced hepatocellular carcinoma. N Engl J Med 2008;359:378-90.

46) Sprinzl MF, Reisinger F, Puschnik A, Ringelhan M, Ackermann K, Hartmann D et al. Sorafenib perpetuates cellular anticancer effector functions by modulating the crosstalk between macrophages and natural killer cells. Hepatology 2013;57:2358-68.

Author names in bold designate shared co-first authorship.

Legends.

Figure 1. Peripheral NK cells of HCC patients show an exhausted phenotype in HCC patients and NKp30-expressing NK cells are enriched in tumor-infiltrating lymphocytes. Frequencies of circulating NK cells, $CD56^{bright}$ and $CD56^{dim}$ subsets (A), NKp30+ NK cells and NKp30-MFI (B-C) in HCC patients (n=55) and HC (n=39). Frequencies of circulating Tim-3 (D), NKG2D (E) and CD69 (F) expressing NK cells in HCC patients (n=14, n=47 and n=44, respectively) and HC (n=10, n=38 and n=34, respectively). Middle bars represent median values, box plots are 25% and

512 75% percentiles, whiskers are minimum and maximum values. The Mann-Whitney U test or the
513 unpaired t test were used to compare data.

514 **Figure 2. Increased proportion of NKp30 receptor-positive NK cells and NKp30 density in**
515 **TIL-NK cells of HCC patients.** The frequency of total NK cells in TIL (n=23) was lower
516 compared with matched LIL (A), with a relative increase of NKp30+ NK cells (B) and NKp30
517 receptor density (C). (D), Representative dot plots showing the frequencies of NKp30-positive NK
518 cells in LIL and matched TIL. (E), Frequency of NKp30-expressing LIL and TIL-NK cells within
519 the $CD56^{bright}$ and $CD56^{dim}$ subsets (n=18). Middle bars represent median values, box plots are 25%
520 and 75% percentiles, whiskers are minimum and maximum values. The Wilcoxon matched-pairs
521 signed rank test or paired t test were used to compare data.

522 **Figure 3. Deficient NKp30-mediated function in HCC patients.** (A), NKp30-mediated
523 degranulation in unstimulated or IL15-stimulated PBMC of HCC patients (n=30), HC (n=29) and
524 HCV+ patients (n=11). (B), NKp30-mediated cytokine production in unstimulated or IL15-
525 stimulated PBMC of HCC patients (n=11), HC (n=15) and HCV+ patients (n=11). NKp30-
526 mediated degranulation (C) and NKp30-mediated cytokine production (D) in unstimulated or IL15-
527 stimulated LIL and matched TIL-NK cells (n=13). Middle bars represent median values, box plots
528 are 25% and 75% percentiles, whiskers are minimum and maximum values. The Mann-Whitney U
529 test, unpaired t test or the Wilcoxon matched-pairs signed rank test were used to compare data.

530 **Figure 4. Altered NKp30 isoform balance in HCC patients**. Relative expression of NKp30
531 isoforms (A) and NKp30 Δac, Δbc and Δab ratios (B) in PBMC of 15 HC and 33 HCC patients. (C),
532 NKp30c isoform expression in HCC patients with stratified according to BCLC staging
533 classification. (D), The Pearson correlation coefficient was used to examine dependence between
534 NKp30 a/c isoform ratio and NKp30-mediated IFNγ production upon IL-15 stimulation, in 19 HCC
535 patients. The relative expression of NKp30 isoforms (E) and the NKp30 Δac, Δbc and Δab ratios (F)
536 were determined in LIL and matched TIL-NK cells from 19 HCC patients.

Figure 5. Cytokine profile in HCC and non-neoplastic tissue. IL-6, IL-8, IL-10, IL-18 and TGF-β mRNA expression on HCC tissues compared with matched non-neoplastic surrounding tissue (n=11). The Wilcoxon matched-pairs signed rank test was used for comparison.

Figure 6. NKp30 is down-regulated after co-culture with a B7-H6 positive HCC cell line. (A), B7-H6 expression on uninfected or HCV-infected Huh7.5 cell line. (B), Frequency of NKp30+ NK cells (B) and NKp30 MFI (C) in HC PBMC (n=11) cultured alone or co-cultured with uninfected or HCV-infected Huh7.5 cell line. (D), B7-H6 expression on HepG2 cells transfected with B7-H6- and or control-siRNA. The frequency NKp30+ cells (E) and NKp30 expression (F) after exposure of PBMC from 10 HC to siRNA-B7-H6-transfected HepG2 cells, siRNA control-transfected HepG2 cells and medium alone. The paired t test was used to compare data.

Figure 7. B7-H6 protein expression is reduced on neoplastic tissue in HCC patients. (A), Immunohistochemical analysis of B7-H6 protein expression on HCC tissue stratified according to degree of differentiation compared to cirrhotic livers (n=28). Data are presented as mean values ± SEM. The Dunn's Multiple Comparison test was used to compare data, ***P<0.001. WD-HCC= well differentiated HCC (n=18), MD-HCC= moderately differentiated HCC (n=34), PD-HCC= poorly differentiated HCC (n=5). (B), Representative B7-H6 and matched negative control or haematoxylin-eosin immunohistochemistry staining on cirrhotic samples and HCC tissue classified as WD-, MD- and PD-HCC (100x magnification). (C), mRNA B7-H6 expression on HCC tissues along with matched non-neoplastic specimens (n=11). The Wilcoxon matched-pairs signed rank test was used. Not statistically significant (ns).

Figure 8. Soluble B7-H6 protein correlates with clinical parameters and is higher in patients with BCLC stage ≥B. (A), Serum B7-H6 concentrations in HCC patients stratified according to BCLC stage (n=87), cirrhotic patients (n=39) and HC (n=48). Data are presented as mean values ± SEM. The Dunn's Multiple Comparison test was used to compare data, *P<0.05, ***P<0.001. The Pearson correlation coefficient was used to examine dependence between sB7-H6 protein (B) and maximum nodule size or sAFP (C), in HCC patients.

HEP-18-0197_R1

Deficient natural killer cell NKp30-mediated function and altered NCR3 splice variants in hepatocellular carcinoma

Stefania Mantovani*[1], Barbara Oliviero*[1], Andrea Lombardi[2,3], Stefania Varchetta[1], Dalila Mele[1], Angelo Sangiovanni[4], Giorgio Rossi[5], Matteo Donadon[6], Guido Torzilli[6], Cristiana Soldani[6], Camillo Porta[7], Paolo Pedrazzoli[7], Silvia Chiellino[7], Roberto Santambrogio[8], Enrico Opocher[8], Marcello Maestri[9], Stefano Bernuzzi[10], Armando Rossello[11], Sophie Clément[3], Claudio De Vito[3], Laura Rubbia-Brandt[3], Francesco Negro[3,12], Mario U Mondelli[1,2].

***Stefania Mantovani and Barbara Oliviero contributed equally to this work.**

[1]Division of Infectious Diseases and Immunology, Department of Medical Sciences and Infectious Diseases, Fondazione IRCCS Policlinico San Matteo, Pavia, Italy. [2]Department of Internal Medicine and Therapeutics, University of Pavia, Italy. [3] Division of Clinical Pathology, University Hospitals, Geneva, Switzerland. [4] CRC "A. M. and A. Migliavacca" Center for Liver Disease, Division of Gastroenterology and Hepatology and [5]Liver Transplant Unit, Fondazione IRCCS Cà Granda Ospedale Maggiore Policlinico, University of Milan, Milan, Italy. [6]Department of Hepatobiliary and General Surgery, Humanitas Clinical and Research Center, Humanitas University, Milan, Italy. [7]Medical Oncology, Fondazione IRCCS Policlinico San Matteo, Pavia, Italy.[8]Division of Gastrointestinal Surgery, San Paolo Hospital, University of Milan School of Medicine, Milan, Italy. [9]Department of General Surgery, Fondazione IRCCS Policlinico San Matteo, Pavia, Italy. [10]Immunohematological and Transfusional Service and Centre of Transplantation Immunology, Fondazione IRCCS Policlinico San Matteo, Pavia, Italy, [11] Department of Pharmacy, University of Pisa, Italy, [12]Division of Gastroenterology and Hepatology, University Hospitals, Geneva, Switzerland.

Table of contents

Supplementary materials and methods.

Study Subjects.

A written informed consent was obtained from each individual. The study protocol is compliant with the ethical guidelines of the 1975 Declaration of Helsinki and was approved by our institutional ethical committee (protocol numbers: 20160004446, 20150000576, 201430031379).

Liver resections.

Surgically resected HCC specimens along with matched non-neoplastic surrounding tissue were obtained from patients at Fondazione IRCCS Policlinico San Matteo, Pavia, Fondazione IRCCS Ca' Granda Policlinico Hospital, Humanitas Research Hospital IRCCS and San Paolo Hospital, Milan. Tissue samples were stored in tissue storage solution (Miltenyi Biotec, Bergisch Gladbach, Germany) or RNA later (Sigma-Aldrich, St. Louis, MO, USA).

Isolation of tissue-infiltrating lymphocytes.

Tissue samples were treated by enzymatic and mechanical dissociation with the human Tumor Dissociation Kit by gentleMACS Dissociator (Miltenyi Biotec), according to the manufacturer's instructions. The cell suspension was filtered in a 70µm cell strainer (Miltenyi Biotec) and centrifuged twice at 50g for 2 min. The supernatant containing lymphocytes was processed for flow cytometry or cryopreserved in liquid N_2.

HCC primary cell cultures.

To establish in-vitro primary tumor cell cultures, the cell pellet was plated in tissue culture flasks (Corning, NY, USA) with Dulbecco's Modified Eagle Medium (Thermo Fisher Scientific, Waltham, MA, USA) supplemented with 20% fetal bovine serum (FBS, HyClone, GE Healthcare, South Logan, Utah, USA), 1% antibiotic antimycotic solution (100 U/ml penicillin, 0.1 µg/ml streptomycin, 0.25 µg/ml amphotericin B) (Sigma-Aldrich) and 1% non-essential amino acids (Thermo Fisher Scientific).

ELISA.

Serum concentrations of soluble B7-H6 were measured by ELISA (EIAab, Wuhan, China) in patients with HCC, cirrhosis and HC, according to the manufacturer's instructions.

Flow cytometry and functional analysis.

Peripheral blood mononuclear cells (PBMC) were isolated from HCC patients and HC by standard methods. Flow cytometry analysis of *ex-vivo* isolated PBMC, non-tumour liver-infiltrating lymphocytes (LIL), tumour-infiltrating lymphocytes (TIL) and PBMC after co-culture with cell lines, was performed using a CyAn (Beckman Coulter, Brea, CA) and a FACSCalibur (Becton Dickinson, Franklin Lakes, NJ) instruments The following mouse anti-human fluorescent antibodies were used: CD16-PE (Becton Dickinson), CD3-FITC (ImmunoTools, Friesoythe, DE), CD56-Pc5.5 (Beckman Coulter), CD56-Pc5 (Beckman Coulter), NKp30-Alexa Fluor®647 (BioLegend, San Diego, CA), NKp30-PE (Becton Dickinson), NKp46-Brilliant Violet 421™ (Becton Dickinson), CD3-PacBlue (Becton Dickinson), NKG2A-APC (Beckman Coulter), CD69-PE (Becton Dickinson), TIGIT-PE (Becton Dickinson), Tim3-PE (Becton Dickinson), FASL-PE (BioLegend), PD-1-APC (Becton Dickinson), NKG2D-APC (Beckman Coulter), CD14-FITC (ImmunoTools), CD3-Alexa Fluor®647 (Becton Dickinson), B7-H6-APC (R&D, Minneapolis, USA). Briefly, $2x10^5$ PBMC were stained with mAb for 30 min at 4°C, washed, immediately fixed in CellFix solution (Becton Dickinson) and analysed. Lymphocytes were identified by the characteristic forward scatter (FSC) and side scatter (SSC) parameters. Total NK cells and NK cell subsets were identified as a CD56+ population within the CD3 negative gate. The proportions of receptor positive cells s were expressed as the frequency of cells of the CD3-CD56+ gated population. Functional redirecting assay, also named reverse antibody-dependent cellular cytotoxicity (ADCC) assay, was performed after cross-linking of NKp30 and FcγR+ P815 murine cell line as previously described [(1)]. Briefly, PBMC, TIL and LIL were incubated overnight with or without IL-15 (20ng/ml, PeproTech EC, London, UK) and subsequently washed and incubated for 4 hours at 37°C with FcγR+ P815 murine target cells (E:T=1:1) in the presence of anti-NKp30 specific mAb (R&D), anti- CD107a-PE (Becton Dickinson) and the Protein Transport Inhibitor

GolgiStop (Becton Dickinson). After washing, lymphocytes were stained for surface NK cell markers using CD3- Brilliant Violet 421™ (Becton Dickinson) and CD56-Pc5.5 (Beckman Coulter). Cells were fixed with BD Cytofix/Cytoperm and permeabilized with the BD Perm/Wash buffer (Becton Dickinson) according to the manufacturer's instructions, in the presence of IFNγ-Alexa Fluor®647 (Becton Dickinson) and TNFα-Alexa Fluor®488 (Becton Dickinson). LIVE/DEAD® Fixable Near-IR Dead Cell Stain Kit (Thermo Fisher Scientific) was used to determine the viability of the cells. Data analysis was performed with the Kaluza 1.3 software (Beckman Coulter).

Immunohistochemistry.

Liver samples from HCC patients and cirrhotic patients were retrospectively collected at the Division of Clinical Pathology, Geneva University Hospitals, Geneva and at Fondazione IRCCS Ca' Granda Policlinico Hospital, University of Milan, Milan. Liver samples were formalin-fixed, paraffin-embedded and processed for histological staining. Serial 4 μm sections were deparaffinised, rehydrated and antigen-retrieval technique was performed with a pH 6 citrate solution in a pressure cooker for 30 min. After blocking of endogenous peroxidase with DAKO REAL Peroxidase-Blocking Solution (Agilent Technologies, Santa Clara, CA, USA), sections were incubated for 1h at room temperature with a rabbit polyclonal B7-H6 antibody (Abcam, Cambridge, UK) diluted 1:250 in DAKO Real Antibody Diluent (Agilent Technologies). After two 5-min washes in DAKO Washing Buffer (Agilent Technologies), sections were incubated for 15 min at room temperature with labelled polymer-HRP and the secondary antibody from the EnVision + Dual Link System-HRP (DAB+) kit (Agilent Technologies). Sections were briefly washed and incubated with 3,3'-diaminobenzidine (DAB) solution (Agilent Technologies) for 120” and the nuclei were visualized by hemalum staining (Merck, Darmstadt, Germany). Prepared slides were preserved by using the Eukitt mounting medium (Kindler, Freiburg, Germany). All specimens were incubated with PBS instead of primary antibody as negative control. The intensity of B7-H6 staining was evaluated in a double-blind fashion by two expert pathologists and classified

evaluating the percentage of cells that stain by immunohistochemistry (on a scale of 0 to 5) and the intensity of that staining (on a scale of 0 to 3), for a possible total score of 8 (AIIRed score) [(2)]. To validate the specificity of the rabbit polyclonal B7-H6 antibody we used western blotting method with a B7-H6 positive breast carcinoma cell line. Briefly, the breast carcinoma cell lines MCF-7/VC and MCF-7/B7-H6 (retrovirally transduced with pMXneo or pMXneo-CD8L-Myc tag-B7-H6 respectively) were kindly provided by Adelheid Cerwenka, Heidelberg, Germany. They were maintained in Dulbeccos's modified Eagle's medium supplemented with 1% GlutaMAX (Thermo Fisher Scientific), 10% fetal cow serum (Thermo Fisher Scientific) and 1% penicillin/streptomicine (Thermo Fisher Scientific). Cells were washed three times with phosphate-buffered saline (PBS) and then lysed in lysis buffer containing 62.5mM Tris-HCl (pH 6.8), 25% glycerol, 2% SDS, 0.02% bromophenol blue, 5% β-mercaptoethanol, protease inhibitors (Roche, Basel, Switzerland), 0.5µl/ml PMSF (Sigma-Aldrich) and 0.5µl/ml sodium orthovanadate. Equal amounts of protein were separated by Sodium Dodecyl Sulphate - PolyAcrylamide Gel Electrophoresis and transferred to the polyvinylidenedifluoride membrane. Non-specific binding sites were blocked with 5% non-fat dry milk in Tris-buffered saline. Membranes were incubated overnight at 4°C with 1:250 dilution of rabbit polyclonal B7-H6 antibody (Abcam, Cambridge, UK) and 1:1000 dilution of mouse monoclonal β-actin antibody (Sigma-Aldrich). Goat anti-rabbit (Licor, Nebraska, USA) and goat anti-mouse (Licor) were used as secondary antibodies. Protein signal was visualized by Odissey system (Licor).

HCV Replication System.

Huh7.5 cells and Japanese fulminant hepatitis HCV genotype 2a strain JFH-1 clone (pJFH-1) were kindly provided by T. Wakita (National Institute of Infectious Diseases, Tokyo, Japan) and grown as previously described [(3)]. HCV RNA transfection was achieved by electroporation with genomic HCV RNA transcribed *in vitro* from pJFH-1, as previously described [(4)]. Culture medium was collected, concentrated 30-fold using Amicon Ultra-15 device (Molecular weight cut off: $1x10^5$ Da, Merck), stored at -80°C and subsequently used to infect naïve Huh7.5 cells. Briefly, naïve Huh 7.5

cells were seeded at a density of 1×10^6 in T75 tissue culture flask, infected overnight with 1×10^6 copies of culture-derived HCV (HCVcc), and analyzed after four and six days by flow cytometry or immunofluorescence for HCV protein expression using human mAb B12.F8 specific for HCV core [5]. After four days in culture, HCV core expression of HCV-infected Huh 7.5 cells was >98% in all cases. Copy numbers of HCV RNA in culture medium were determined by quantitative real-time PCR (qPCR). Total RNA was isolated from 100 µl of concentrated culture supernatant with the QIAamp MinElute Virus Spin Kit (Qiagen, Hilden, Germany) and qPCR was performed with AgPAth-ID One-Step RT-PCR Kit (Thermo Fisher Scientific) and the CFX96 Real-Time machine detection system (BioRad, Hercules, CA, USA) according to manufacturer's instructions and relative to a standard curve comprised of serial dilutions of JFH-1 plasmid. The forward and reverse primers were 5′-TCCCGGGAGAGCCATAGTG-3′ and 5′-GCACCCTATCAGGCAGTACCA-3′, respectively. The TaqMan probe was 5′-6(FAM)-TCTGCGGAACCGGTG-MGB-3′ (Thermo Fisher Scientific).

RNA extraction and qPCR.

Expression of major NKp30 isoforms was quantified by real-time PCR (qPCR) and normalized to β2-microglobulin gene in PBMC of HCC patients, HC and in TIL and LIL as previously described [6]. Expression of the distinct NKp30 isoforms compared with each other (Δ) was determined using the following formula $\Delta NKp30_x$ $NKp30_y = C_tNKp30_y - C_tNKp30_x$. NKp30 isoform ratio was determined by the following formula: $NKp30_x/NKp30_y = 2^{(\Delta\Delta CtNKp30y - \Delta\Delta CtNKp30x)}$. Tissue and HepG2 RNA extraction was performed with TRIzol reagent (Thermo Fisher Scientific) using a gentleMACS Dissociator (MiltenyiBiotec) and with RNeasy Plus Mini kit and DNAse treatment on column (Qiagen), following the manufacturer's instructions. First-strand cDNA was synthesized from 5µg of total RNA using SuperScript III reverse transcriptase and random primers, following the manufacturer's instructions (Thermo Fisher Scientific). The Fast SYBR® Green Master Mix (Thermo Fisher Scientific) and the SsoAdvanced Universal SYBR Green Supermix (BioRad) were

used. All reactions were performed using the CFX96 Real-Time machine detection system (BioRad). Each sample was amplified in triplicate and the qPCR data were analysed using the $2^{-\Delta Ct}$ method. B7-H6, IL-6, IL-8, IL-10, IL-18 and TGF-β mRNA expression were evaluated in HCC specimens and surrounding matched non-neoplastic tissue and normalized to glyceraldehyde 3-phosphate dehydrogenase gene. The following primers were used: GAPDH forward 5′-CGGATTTGGTCGTATTGG-3′ and reverse 5′-GGTGGAATCATATTGGAACA -3′ (Primm, Milan, Italy); B7-H6 PrimePCR™ SYBR® Green Assay qHsaCID0016055 (BioRad); IL-6 PrimePCR™ SYBR® Green Assay qHsaCID0020314 (BioRad); IL-8 forward 5'-GACCACACTGCGCCAACAC-3' and reverse 5' CTTCTCCACAACCCTCTGCAC-3' (Thermo Fisher Scientific); IL-18 PrimePCR™ SYBR® Green Assay qHsaCID0006163 (BioRad); TGF-beta PrimePCR™ SYBR® Green Assay qHsaCID0017026; IL-10 forward 5'GCCTAACATGCTTCGAGATC-3' and reverse 5'-TGATGTCTGGGTCTTGGTTC-3' (Thermo Fisher Scientific).

Exposure of PBMC to B7-H6 positive cell lines or to serum containing sB7-H6.

1×10^5 freshly isolated PBMC from HC were co-cultured overnight alone or with 1×10^5 uninfected or HCV-infected Huh7.5 cells expressing the NKp30 B7-H6 ligand. Identical conditions were used to co-culture PBMC with siRNA treated HepG2 cells or the breast carcinoma cell lines MCF-7/VC or MCF-7/B7-H6, retrovirally transduced with pMXneo or pMXneo-CD8L-Myc tag-B7-H6, respectively [7]. B7-H6 expression was evaluated by flow cytometry using anti-human B7-H6 antibody (R&D). 1.5×10^5 freshly isolated PBMC from HC were incubated overnight alone, with serum from heterologous HC and with serum from HCC patients containing sB7-H6. NKp30 expression on NK cells was evaluated by flow cytometry.

siRNA-mediated knockdown.

Silencer® Select siRNA n266791 (Thermo Fisher Scientific), designed to knock down the B7-H6 gene expression, and a Silencer® Select negative control siRNA were used to a final RNA

concentration of 10nM. HepG2 cells were reverse transfected following the manufacturer's instructions. siRNA knockdown was assessed by qPCR and flow cytometry.

Exposure of HCC primary cell lines to ADAM-10 and -17 specific inhibitors.

The selective ADAM-10 and -17 specific inhibitors MN8 and LT4[8] were used. HCC primary cell lines were treated with 2.5 μM to 50 μM of MN8, LT4 or with dimethyl sulfoxide for 24 hours. The modulation of surface B7-H6 expression was verified by flow cytometry using anti-human B7-H6 antibody (R&D).

Supplementary references.

Author names in bold designate shared co-first authorship.

1. Oliviero B, Varchetta S, Paudice E, Michelone G, Zaramella M, Mavilio D, et al. Natural killer cell functional dichotomy in chronic hepatitis B and chronic hepatitis C virus infections. Gastroenterology 2009;137:1151-1160
2. Allred DC , Harvey JM , Berardo M , Clark GM . Prognostic and predictive factors in breast cancer by immunohistochemical analysis . Mod Pathol .1998;11(2):155-168.
3. **Zhong J, Gastaminza P**, Cheng G, Kapadia S, Kato T, Burton DR, et al. Robust hepatitis C virus infection in vitro. Proc Natl Acad Sci U S A 2005;102:9294-9929.
4. Kato T, Date T, Murayama A, Morikawa K, Akazawa D, Wakita T. Cell culture and infection system for hepatitis C virus. Nat Protoc 2006;1:2334-2339
5. Cerino A, Boender P, La Monica N, Rosa C, Habets W, Mondelli MU. A human monoclonal antibody specific for the N terminus of the hepatitis C virus nucleocapsid protein. J Immunol 1993;151:7005-7015
6. Mantovani S, Mele D, Oliviero B, Barbarini G, Varchetta S, Mondelli MU. NKp30 isoforms in patients with chronic hepatitis C virus infection. Immunology 2015;146:234-42.
7. Schlecker E, Fiegler N, Arnold A, Altevogt P, Rose-John S, Moldenhauer G, et al. Metalloprotease-mediated tumor cell shedding of B7-H6, the ligand of the natural killer cell-activating receptor NKp30. Cancer Res 2014;74:3429-40.
8. Camodeca C, Nuti E, Tepshi L, Boero S, Tuccinardi T, Stura EA et al. Discovery of a new selective inhibitor of A Disintegrin And Metalloprotease 10 (ADAM-10) able to reduce the shedding of NKG2D ligands in Hodgkin's lymphoma cell models. Eur J Med Chem 2016;111:193-201.

Supplementary Table 1. Clinical characteristics of patients and controls.

	HC	Cirrhotic patients	HCV patients	HCC patients
Number of subjects	66	95	11	170
Male/Female	44/22	67/28	3/8	133/37
Median age (years) - range	47 (21-86)	56 (29-83)	69 (37-77)	65 (30-85)
ALT (mU/ml) median, range	26 (14-45)	80 (6-281)	70 (12-254)	51 (8-294)
AST (mU/ml), median, range	na*	75 (15-336)	71 (15-187)	66 (17-326)
APRI, median, range	na	1.69 (0.26-8.30)	1.10 (0.15-1.67)	1.62 (0.20-17.63)
FIB-4, median, range	na	3.62 (0.79-24.53)	3.16 (1.35-5.35)	5.08 (0.49-34.04)
Liver stiffness, median, range	na	17.75 (6.80-41.00)	14.50 (7.10-20.90)	na
BCLC score				
A	na	na	na	67
B	na	na	na	32
C	na	na	na	43
D	na	na	na	15
CTP score				
A	na	72	na	107
B	na	22	na	29
C	na	1	na	14
MELD score				
≤15	na	91	na	125
15-20	na	4	na	6
≥20	na	0	na	10
HCC size** (mm), median, range	na	na	na	30 (8-180)
Etiology				
HBV	na	13	0	17
HCV	na	67	11	115
HBV + HCV	na	0	0	3
NASH	na	3	0	7
NASH + Ethanol	na	12	0	2
HBV or HCV + Ethanol	na	0	0	8
Unknown	na	0	0	18

*na: not applicable.

**Maximum nodule width.

ALT, alanine aminotransferase; AST, aspartate aminotransferase; APRI, aspartate aminotransferase to platelet ratio index; FIB-4, fibrosis-4; BCLC, Barcelona Clinic Liver Cancer; MELD, Model for End Stage Liver Disease; CTP, Child-Turcotte-Pugh.

FIG 1

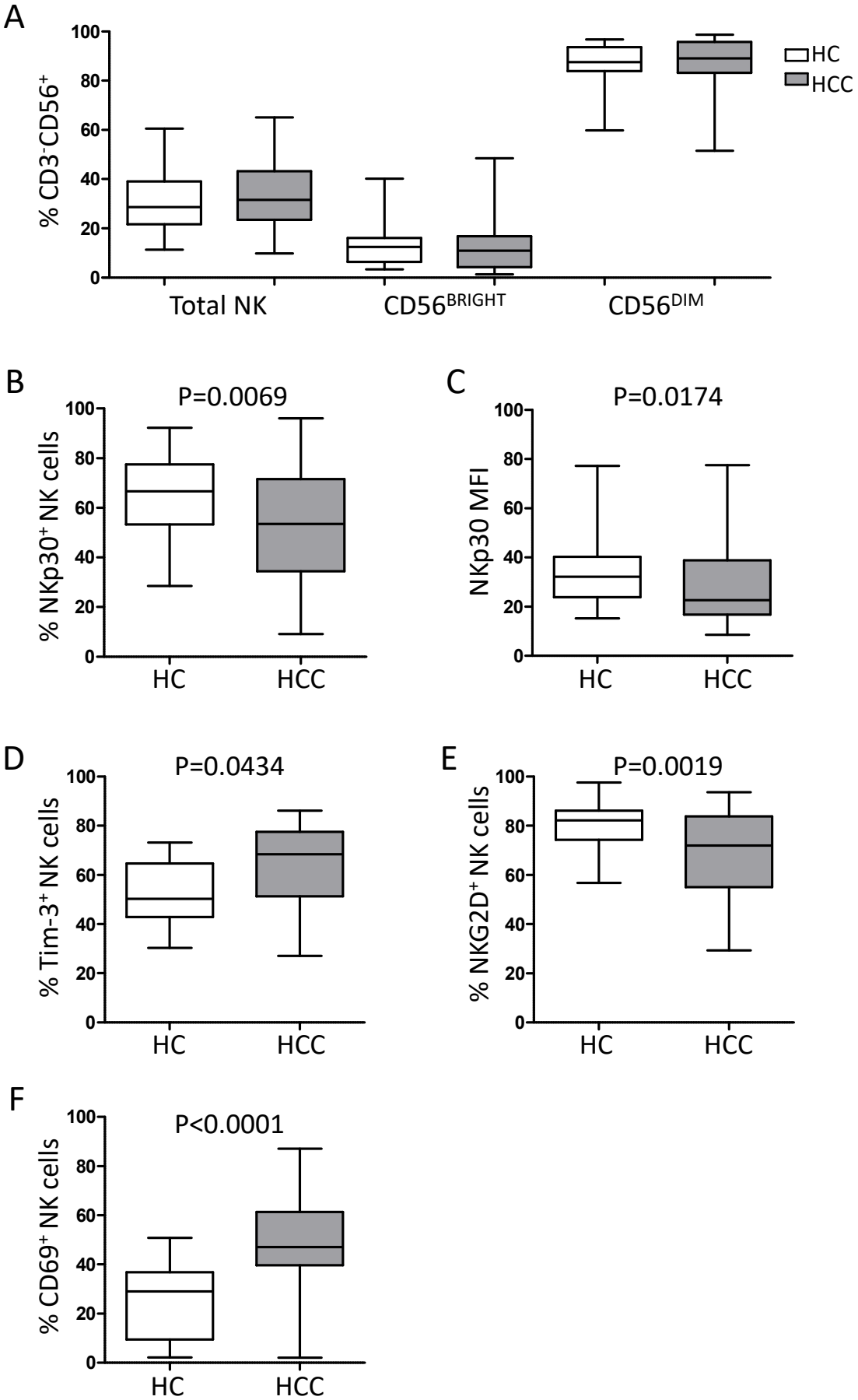
A
% CD3-CD56+
100
80
60
40
20
0
HC
HCC
Total NK
CD56BRIGHT
CD56DIM
B
P=0.0069
% NKp30+ NK cells
HC
HCC
C
P=0.0174
NKp30 MFI
HC
HCC
D
P=0.0434
% Tim-3+ NK cells
HC
HCC
E
P=0.0019
% NKG2D+ NK cells
HC
HCC
F
P<0.0001
% CD69+ NK cells
HC
HCC

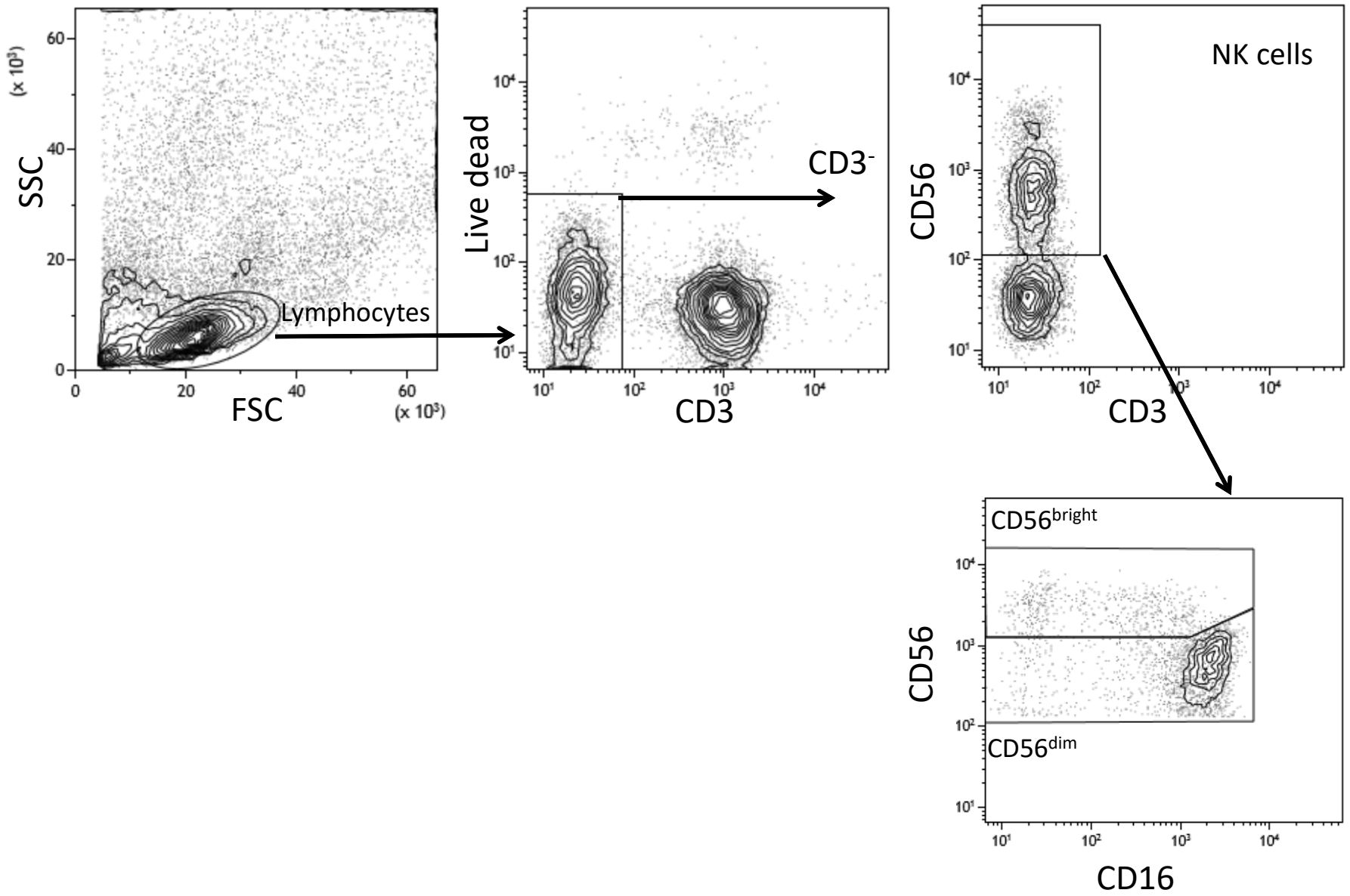

Supplementary Fig. 1. Gating strategy in a representative HCC patient.

FIG 2

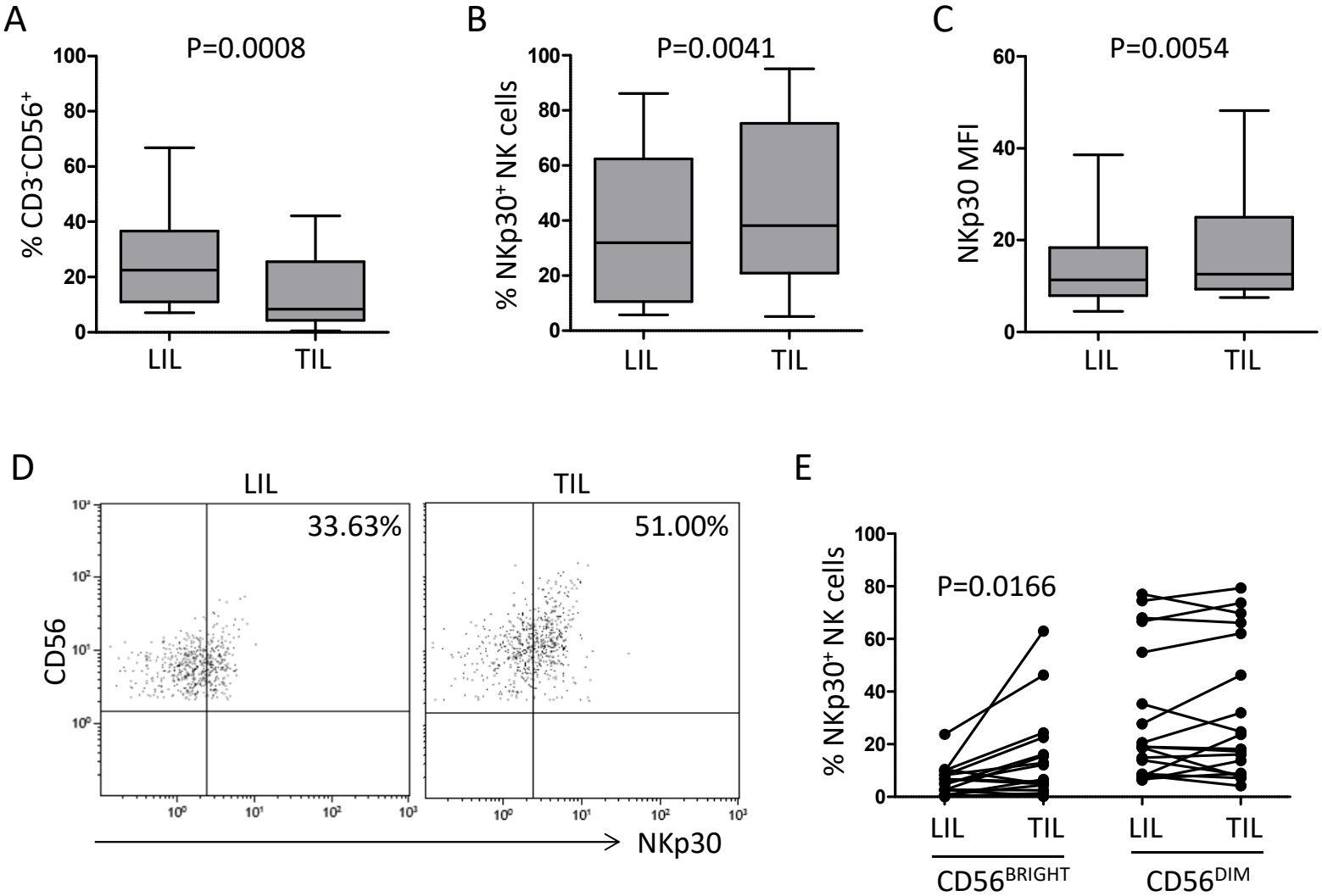
A
P=0.0008
% CD3-CD56+
100
80
60
40
20
0
LIL
TIL
B
P=0.0041
% NKp30+ NK cells
100
80
60
40
20
0
LIL
TIL
C
P=0.0054
NKp30 MFI
60
40
20
0
LIL
TIL
D
LIL
TIL
33.63%
51.00%
CD56
NKp30
E
P=0.0166
% NKp30+ NK cells
100
80
60
40
20
0
LIL
TIL
LIL
TIL
CD56BRIGHT
CD56DIM

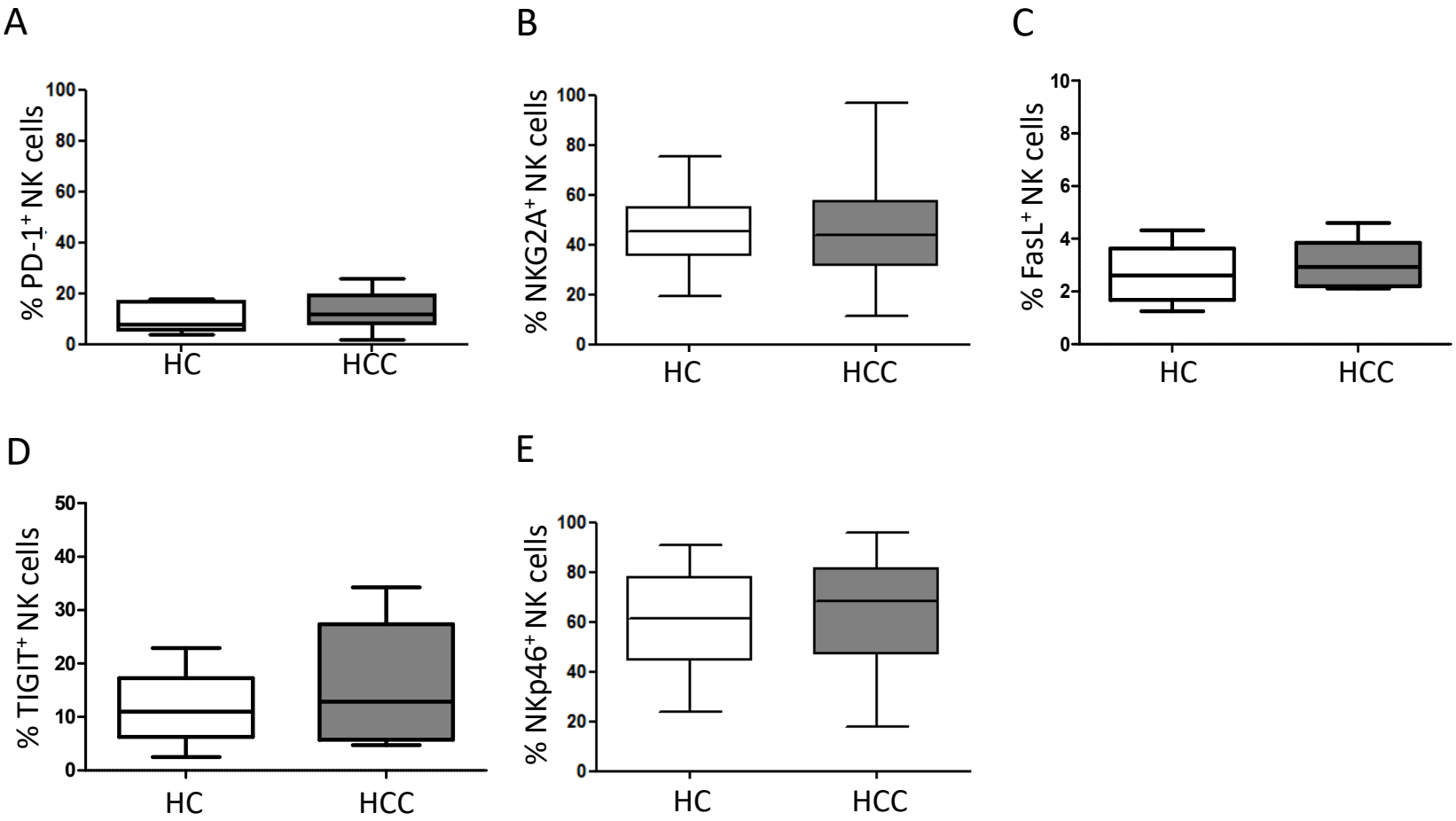

Supplementary Fig. 2. HCC patients were further examined for expression of other molecules, including PD-1 (A, n=14), NKG2A (B, n=44), FasL (C, n=6), TIGIT (D, n=10), NKp46 (E, n=45), simultaneously with HC (A, n= 10; B, n=37; C, n=6; D, n=10; E, n=34). There were no statistically significant differences between patients with HCC and controls. Middle bars represent median values, box plots are 25% and 75% percentiles, whiskers are minimum and maximum values. The Mann-Whitney U test was used to compare data.

FIG 3

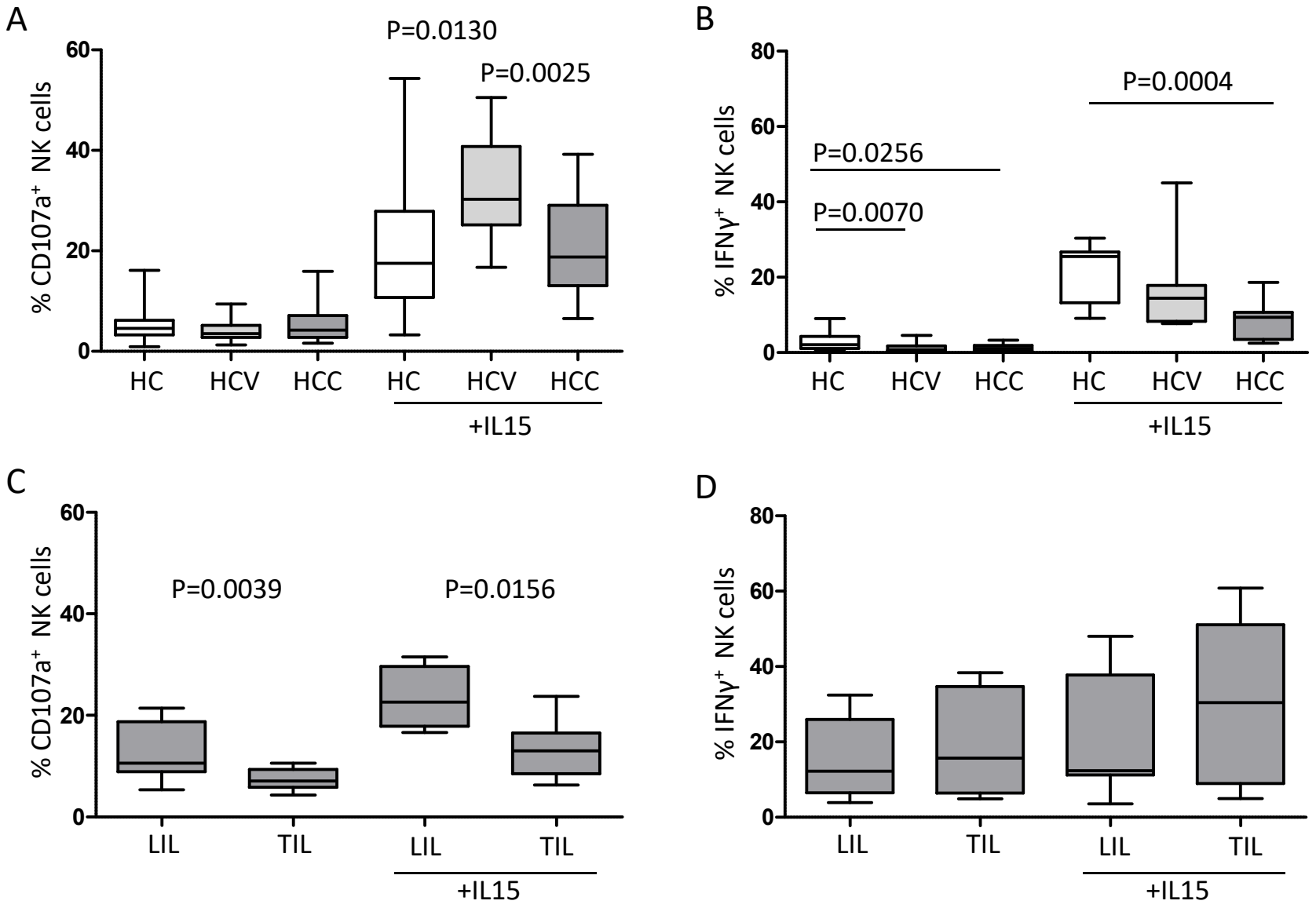
A
P=0.0130
P=0.0025
% CD107a+ NK cells
60
40
20
0
HC
HCV
HCC
HC
HCV
HCC
+IL15
B
P=0.0004
P=0.0256
P=0.0070
% IFNγ+ NK cells
80
60
40
20
0
HC
HCV
HCC
HC
HCV
HCC
+IL15
C
P=0.0039
P=0.0156
% CD107a+ NK cells
60
40
20
0
LIL
TIL
LIL
TIL
+IL15
D
% IFNγ+ NK cells
80
60
40
20
0
LIL
TIL
LIL
TIL
+IL15

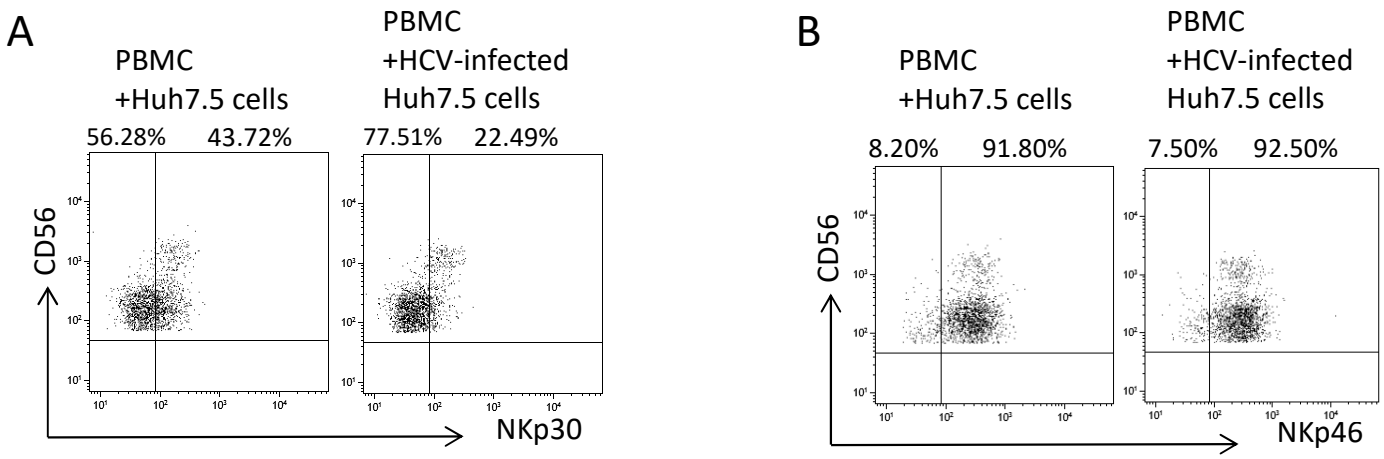

Supplementary Fig. 3. Co-culture experiments with Huh7.5 cells expressing the B7-H6 ligand. Representative flow cytometry dot plots showing NKp30+ (A) and NKp46+ (B) NK cell frequencies after exposure to HCV-infected or uninfected Huh7.5 cells.

FIG 4

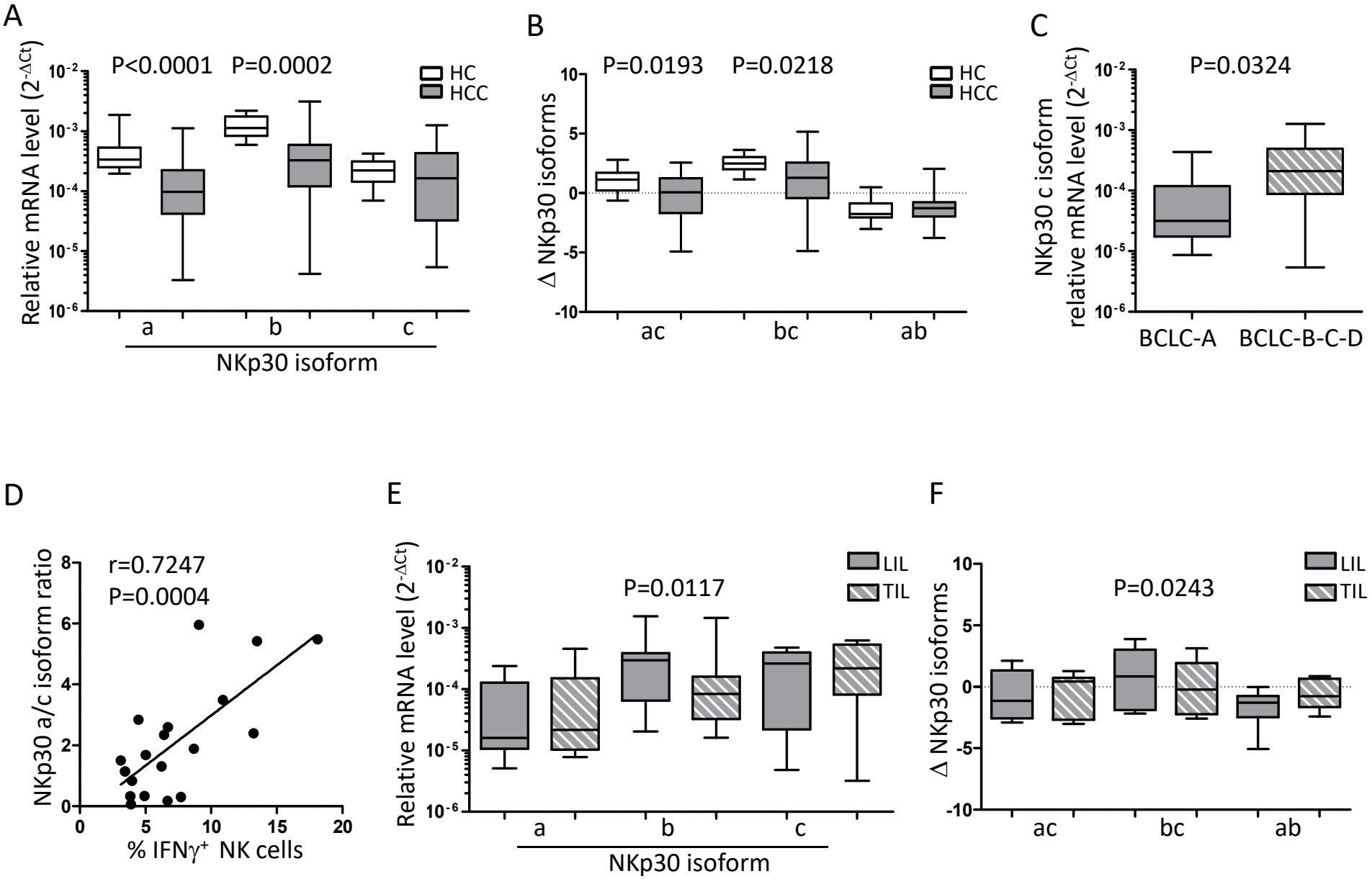
A
P<0.0001
P=0.0002
HC
HCC
Relative mRNA level (2-ΔCt)
a
b
c
NKp30 isoform
B
P=0.0193
P=0.0218
HC
HCC
Δ NKp30 isoforms
ac
bc
ab
C
P=0.0324
NKp30 c isoform relative mRNA level (2-ΔCt)
BCLC-A
BCLC-B-C-D
D
r=0.7247
P=0.0004
NKp30 a/c isoform ratio
% IFNγ+ NK cells
E
P=0.0117
LIL
TIL
Relative mRNA level (2-ΔCt)
a
b
c
NKp30 isoform
F
P=0.0243
LIL
TIL
Δ NKp30 isoforms
ac
bc
ab

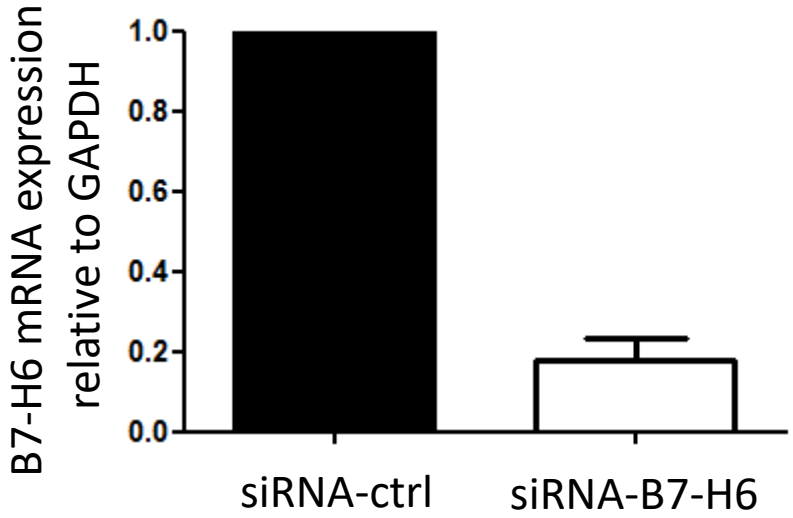

Supplementary Fig. 4. B7-H6 mRNA is reduced following transfection of HepG2 cells with B7-H6 siRNA compared to control siRNA. B7-H6 knock-down in HepG2 cells was determined by RT-PCR. Results are shown as means ± SEM of three independent experiments.

FIG 5

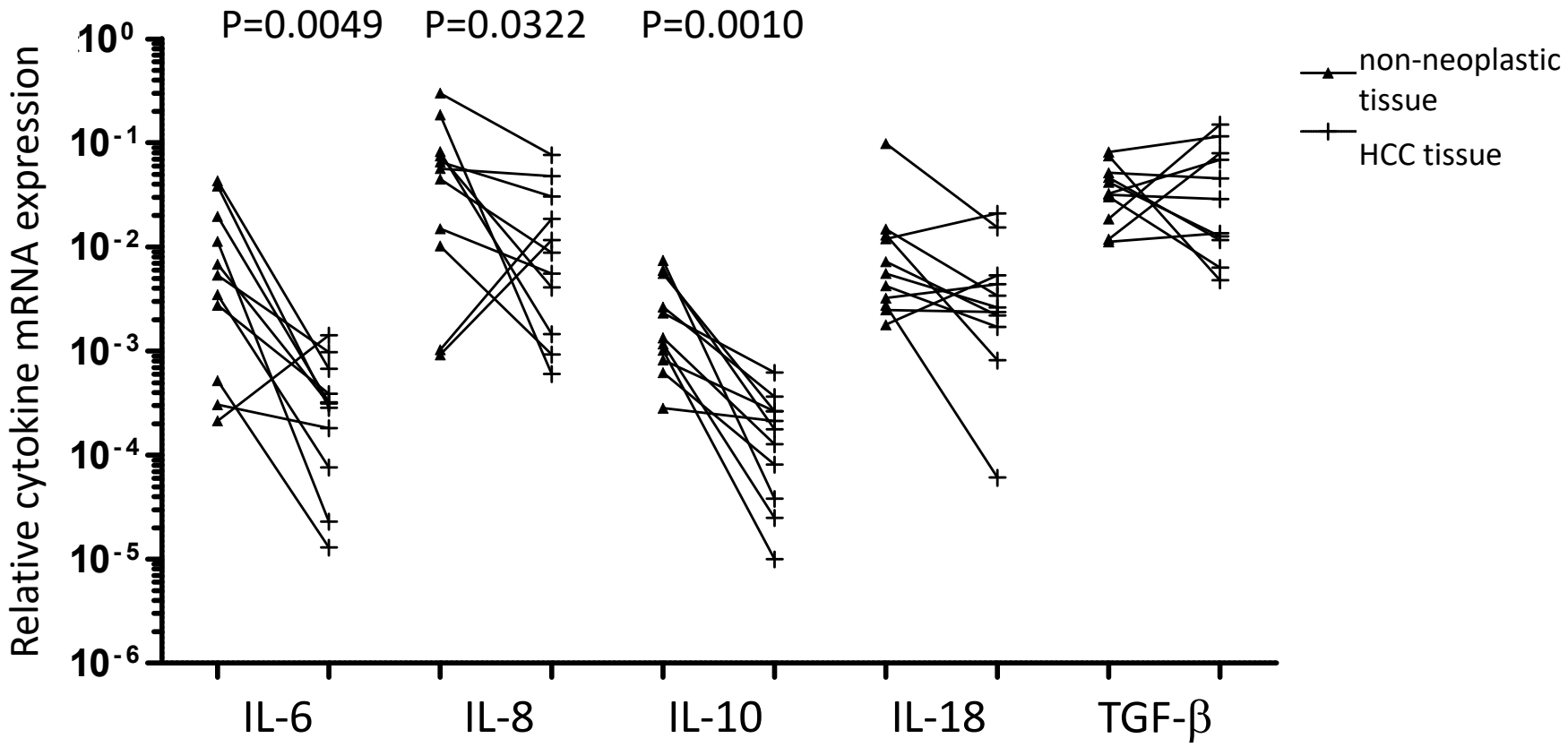
P=0.0049
P=0.0322
P=0.0010
Relative cytokine mRNA expression
10⁰
10⁻¹
10⁻²
10⁻³
10⁻⁴
10⁻⁵
10⁻⁶
IL-6
IL-8
IL-10
IL-18
TGF-β
non-neoplastic tissue
HCC tissue

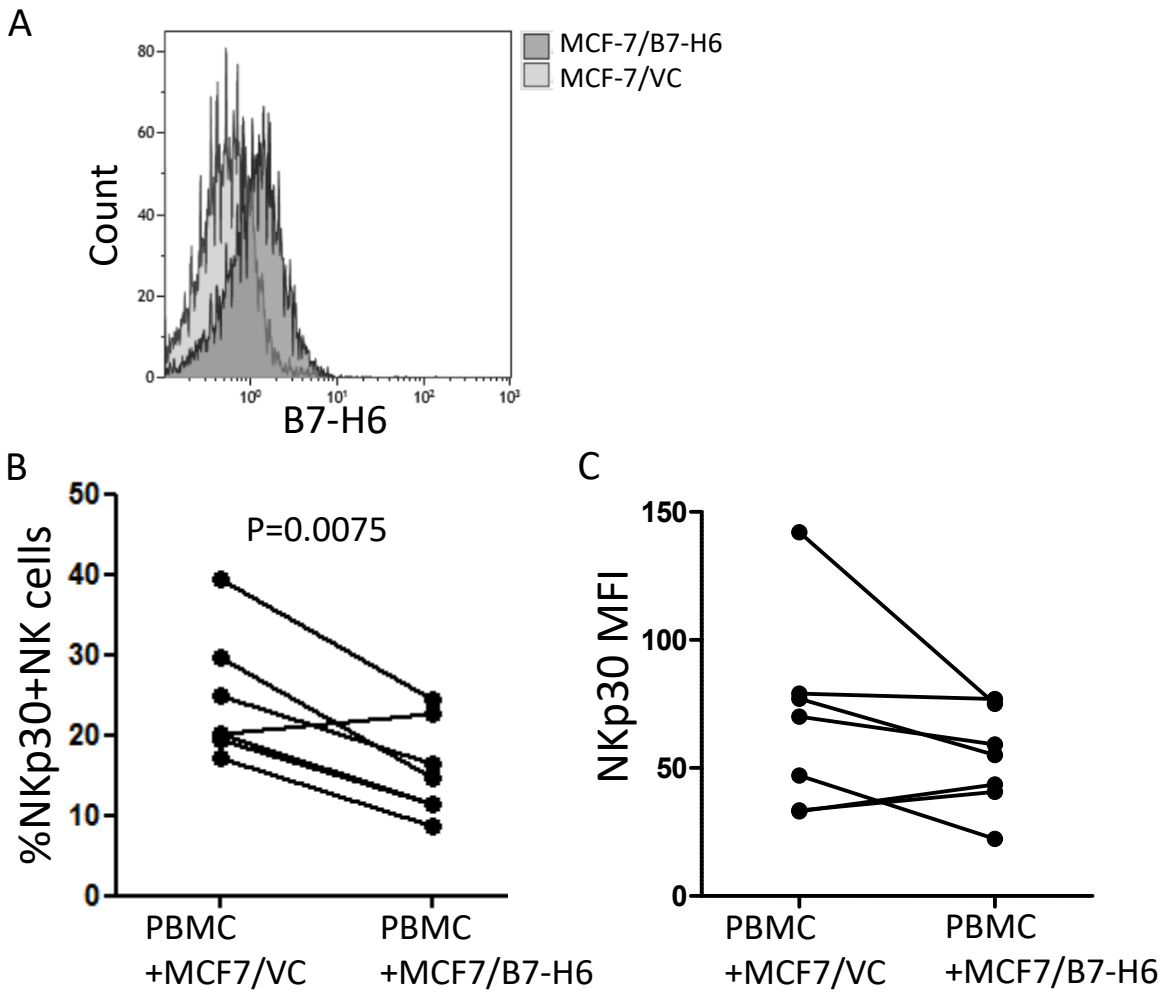

Supplementary Fig. 5. Co-culture of freshly isolated PBMC from HC with breast carcinoma cell lines MCF-7/VC or MCF-7/B7-H6, retrovirally transduced with pMXneo or pMXneo-CD8L-Myc tag-B7-H6, respectively. Flow cytometry was used to evaluate B7-H6 expression on MCF7/VC and MCF-7/B7-H6 cell lines, as shown in panel A. Frequencies (B)of NKp30+ NK cells and NKp30 MFI (C) were evaluated by flow cytometry in PBMC from HC (n=7) after overnight culture with MCF-7/VC or MCF-7/B7-H6 cell lines. The paired t test was used to compare data.

FIG 6

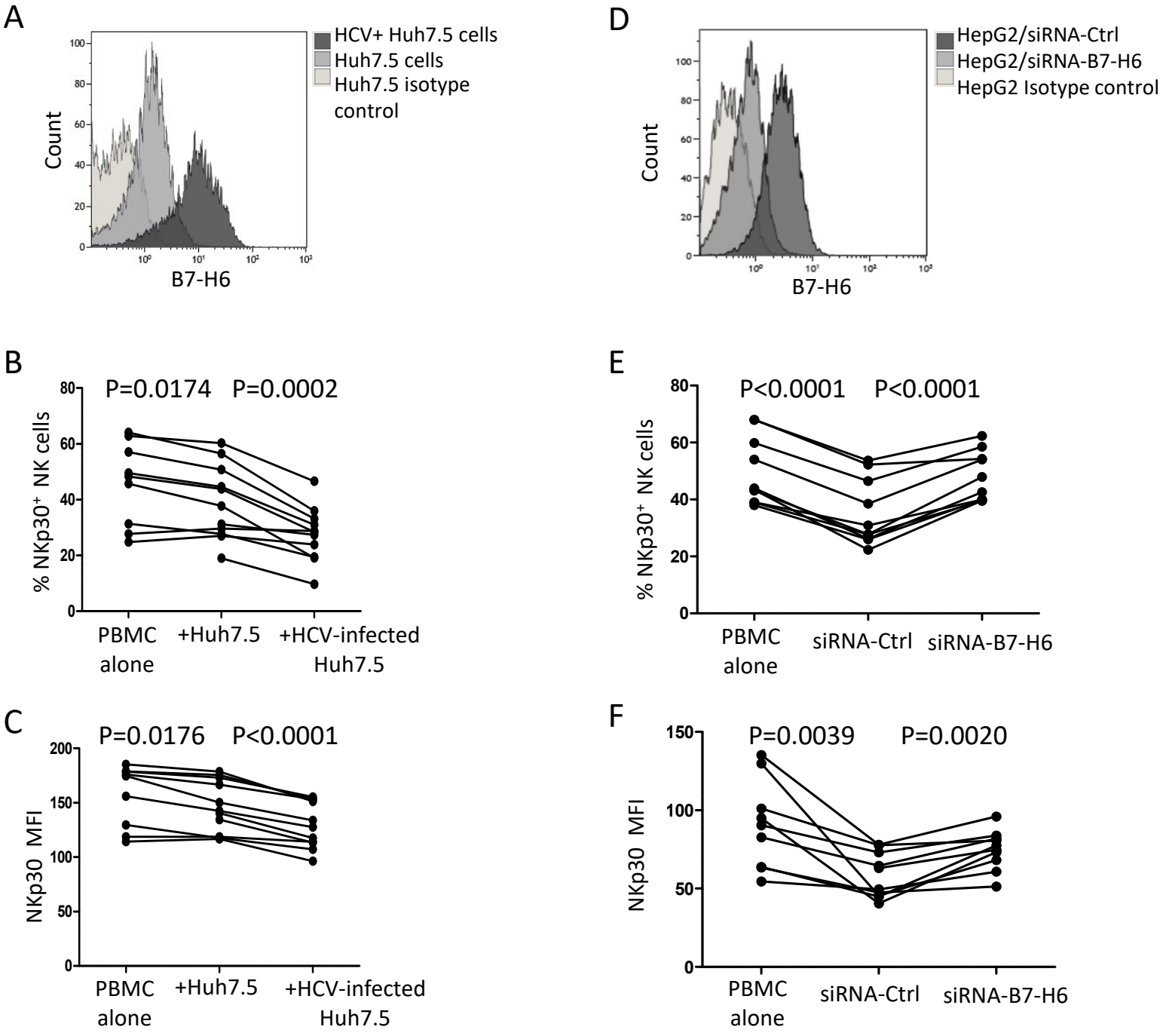
A
HCV+ Huh7.5 cells
Huh7.5 cells
Huh7.5 isotype control
Count
B7-H6
D
HepG2/siRNA-Ctrl
HepG2/siRNA-B7-H6
HepG2 Isotype control
Count
B7-H6
B
P=0.0174 P=0.0002
% NKp30+ NK cells
PBMC alone
+Huh7.5
+HCV-infected Huh7.5
E
P<0.0001 P<0.0001
% NKp30+ NK cells
PBMC alone
siRNA-Ctrl
siRNA-B7-H6
C
P=0.0176 P<0.0001
NKp30 MFI
PBMC alone
+Huh7.5
+HCV-infected Huh7.5
F
P=0.0039 P=0.0020
NKp30 MFI
PBMC alone
siRNA-Ctrl
siRNA-B7-H6

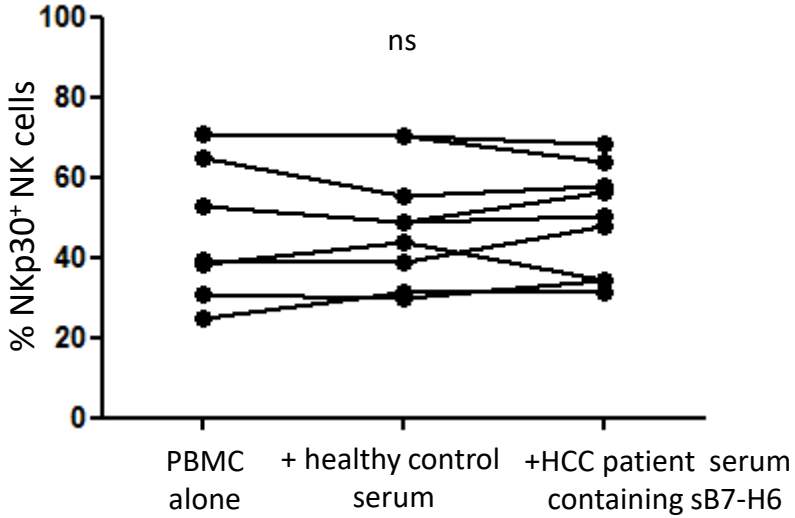

Supplementary Fig. 6. Freshly isolated PBMC from HC were incubated alone or with heterologous serum from healthy controls or HCC patients containing soluble B7-H6. The frequencies of NKp30+ NK cells were evaluated by flow cytometry in HC PBMC (n=9) after overnight incubation. The paired t test was used to compare data.

Fig 7

A

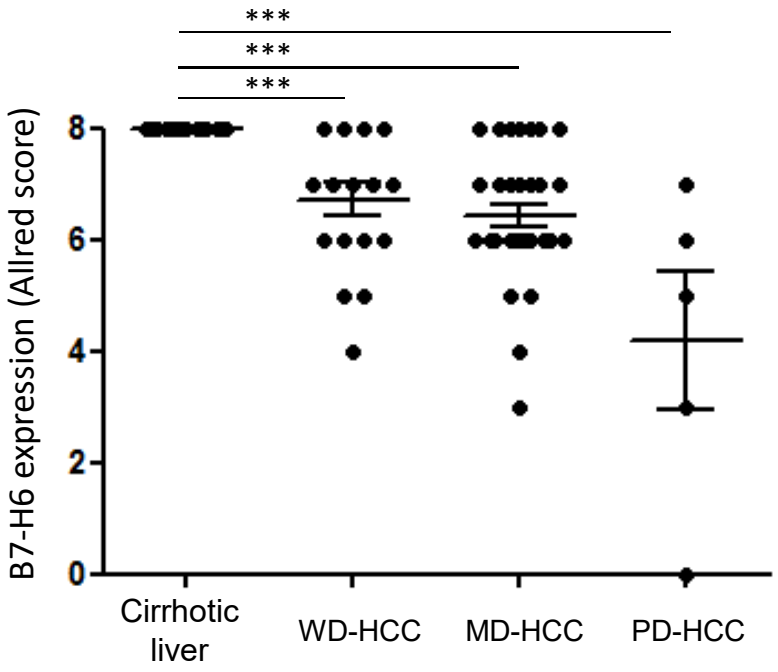
***
***
***
B7-H6 expression (Allred score)
8
6
4
2
0
Cirrhotic liver
WD-HCC
MD-HCC
PD-HCC

B

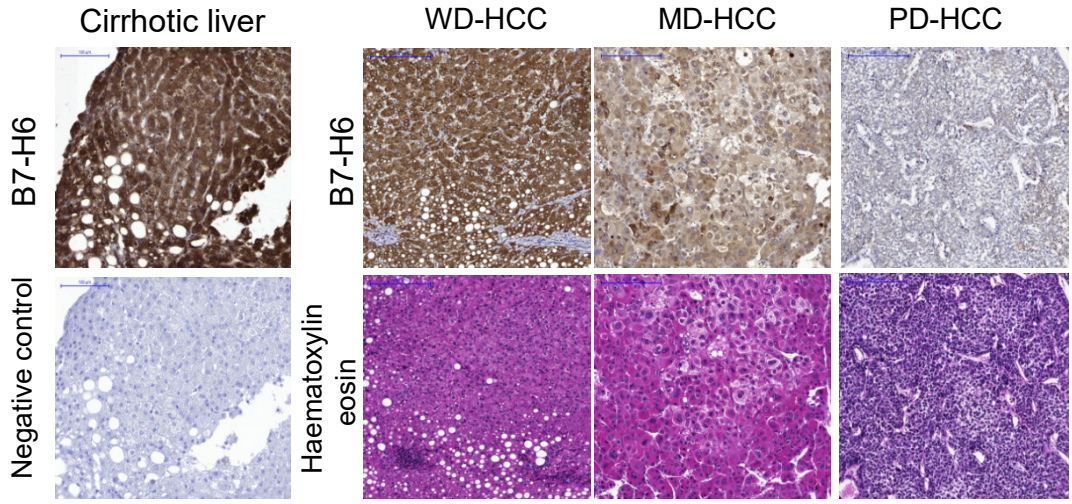
Cirrhotic liver
WD-HCC
MD-HCC
PD-HCC
B7-H6
B7-H6
Negative control
Haematoxylin eosin

C

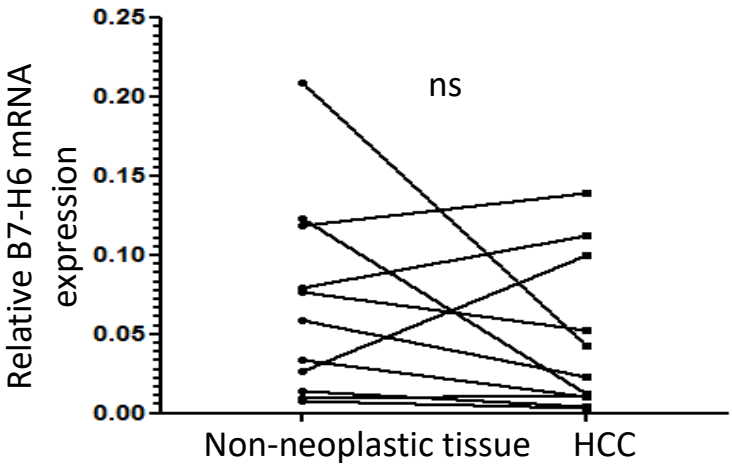
Relative B7-H6 mRNA expression
0.25
0.20
0.15
0.10
0.05
0.00
ns
Non-neoplastic tissue
HCC

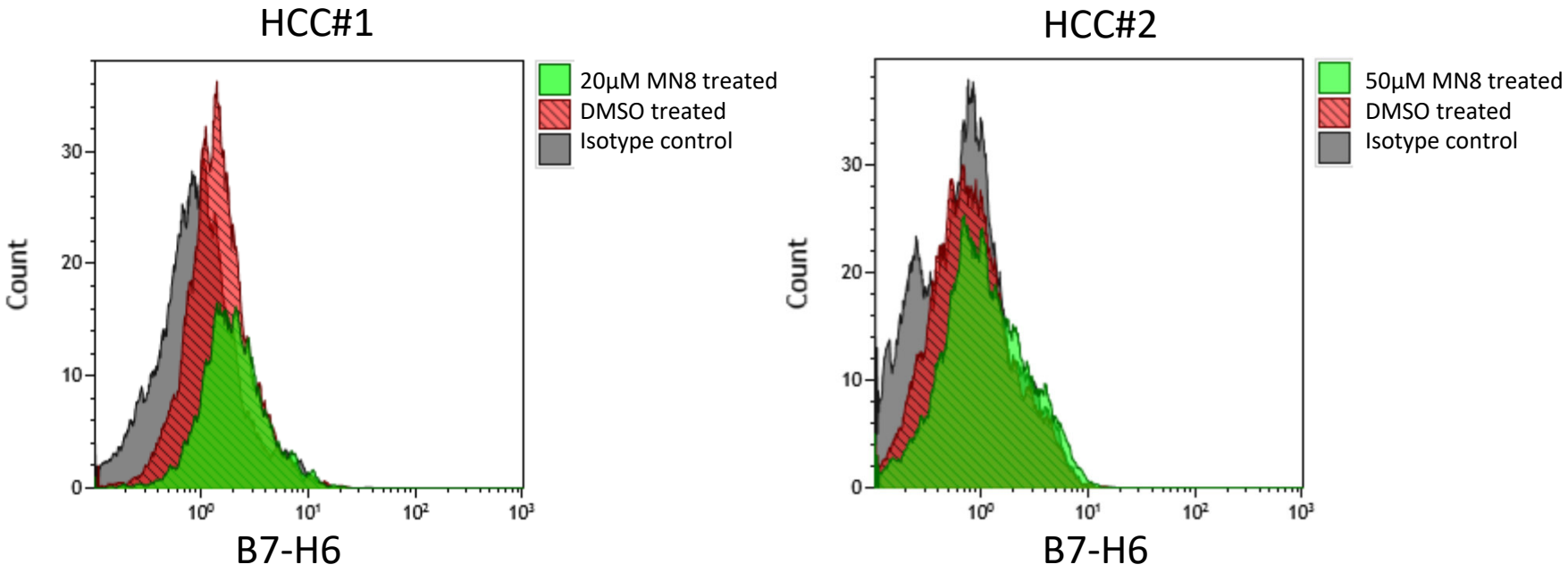

Supplementary Fig. 7. Exposure of HCC primary cell lines to MN8 “A Disintegrin And Metalloproteases” (ADAM)-10 and -17 specific inhibitor.

FIG 8

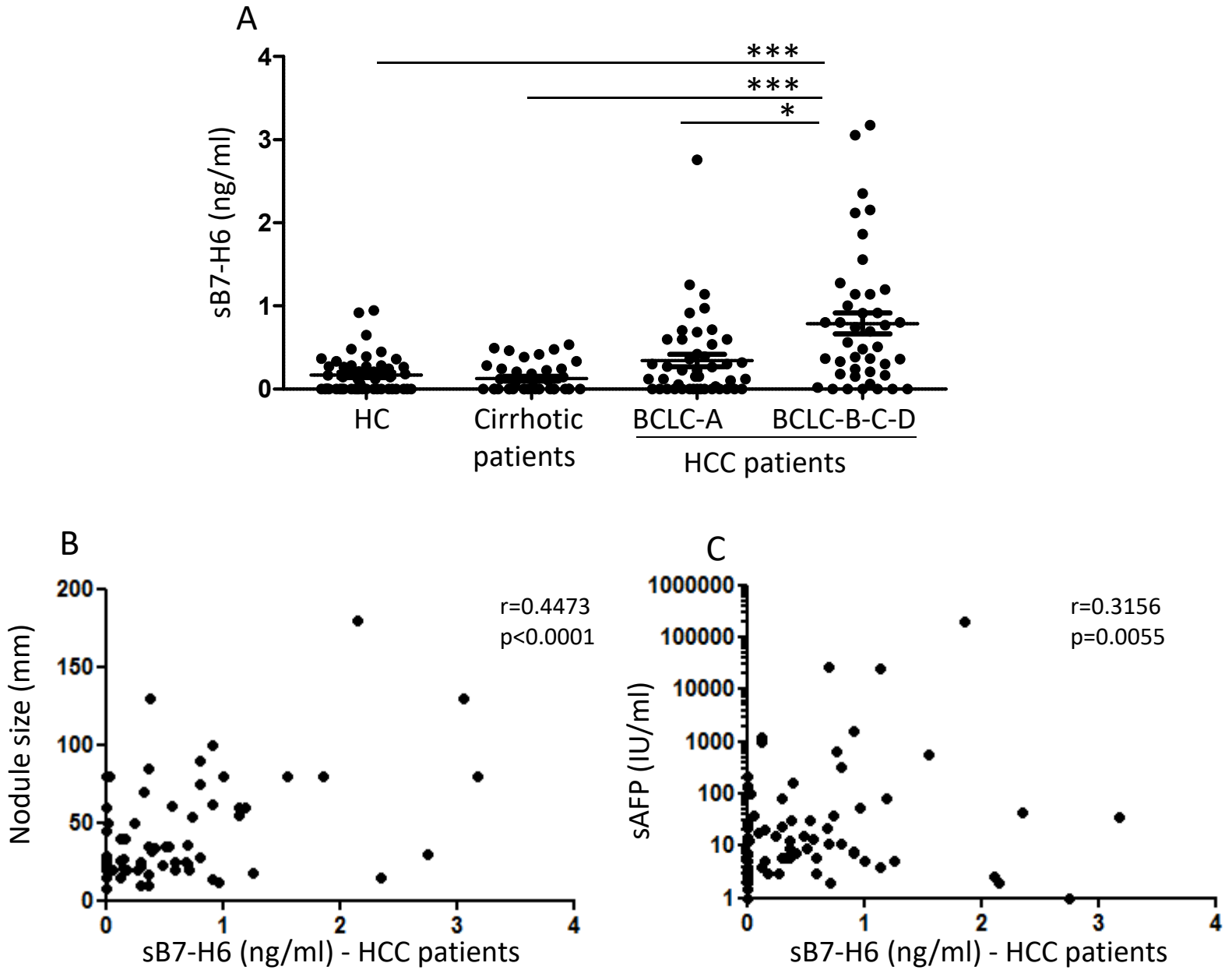
A
***
***
*
sB7-H6 (ng/ml)
4
3
2
1
0
HC
Cirrhotic patients
BCLC-A
BCLC-B-C-D
HCC patients
B
Nodule size (mm)
200
150
100
50
0
r=0.4473
p<0.0001
0
1
2
3
4
sB7-H6 (ng/ml) - HCC patients
C
sAFP (IU/ml)
1000000
100000
10000
1000
100
10
1
r=0.3156
p=0.0055
0
1
2
3
4
sB7-H6 (ng/ml) - HCC patients